AOD distributions and trends of major aerosol species over a selection of the world's most populated cities based on the 1st Version of NASA's MERRA Aerosol Reanalysis

Simon Provençal[1*], Pavel Kishcha[2], Arlindo M. da Silva[3], Emily Elhacham[2] and Pinhas Alpert[2]

[1] Département de géographie, Université Laval, Quebec City, Quebec, Canada
[2] Department of Geosciences, Tel Aviv University, Tel Aviv, Israel
[3] Goddard Space Flight Center, National Aeronautics and Space Administration, Greenbelt, Maryland, USA
[*] Corresponding author: simon.provencal.1@ulaval.ca

Abstract

NASA recently extended the Modern-Era Retrospective Analysis for Research and Application (MERRA) with an atmospheric aerosol reanalysis which includes five particulate species: sulfate, organic matter, black carbon, mineral dust and sea salt. The MERRA Aerosol Reanalysis (MERRAero) is an innovative tool to study air quality issues around the world for its global and constant coverage and its distinction of aerosol speciation expressed in the form of aerosol optical depth (AOD). The purpose of this manuscript is to apply MERRAero to the study of urban air pollution at the global scale by analyzing the AOD over a period of 13 years (2003–2015) and over a selection of 200 of the world's most populated cities in order to assess the impacts of urbanization, industrialization, air quality regulations and regional transport which affect urban aerosol load. Environmental regulations and the recent global economic recession have helped to decrease the AOD and sulfate aerosols in most cities in North America, Europe and Japan. Rapid industrialization in China over the last two decades resulted in Chinese cities having the highest AOD values in the world. China has nevertheless recently implemented emission control measures which are showing early signs of success in many cities of Southern China where AOD has decreased substantially over the last 13 years. The AOD over South American cities, which is dominated by carbonaceous aerosols, has also decreased over the last decade due to an increase in commodity prices which slowed deforestation activities in the Amazon rainforest. At the opposite, recent urbanization and industrialization in India and Bangladesh resulted in a strong increase of AOD, sulfate and carbonaceous aerosols in most cities of these two countries. The AOD over most cities in Northern Africa and Western Asia changed little over the last decade. Emissions of natural aerosols, which cities in these two regions tend to be mostly composed of, don't tend to fluctuate significantly on an annual basis.

Keywords: Urban air pollution; Aerosol optical depth (AOD); Sulfate; Particulate organic matter; Black carbon; Mineral dust; MERRAero.

1 Introduction

Microscopic airborne aerosols have long been a prominent topic of study in the field of environmental science, predominantly in the atmospheric sciences. A considerable amount of literature has emerged in order to better understand the nature of these particles, but more specifically, to assess their impacts on various spheres of life and the environment. Aerosols are found in highly variable space and time distribution, size and chemical composition, and they

originate from many sources, both natural and anthropogenic (Pöschl, 2005).

Aerosols considerably affect the environment and its living organisms. It is well documented that aerosols are a serious health hazard to humans, fauna and flora. They are linked to cardiovascular, respiratory and allergic diseases, as well as enhanced mortality (Pöschl, 2005; Tager, 2013). Aerosols also affect weather and climate. Acting as cloud condensation nuclei, aerosols are an essential element of cloud formation. As such, they play an indirect role in increasing the clouds' and the Earth's albedo as a whole (Haywood and Boucher, 2000; Lohmann and Feichter, 2005). They also affect the Earth's radiation budget as absorbers of radiation, contributing to a warming of the atmosphere, and as reflectors of radiation, in which case they act as a cooling agent (Haywood and Boucher, 2000). Finally, in high enough concentration, they can significantly reduce visibility (Charlson, 1969; Cheng and Tsai, 2000). This is often associated with episodes of haze, smog and dust storms.

The seriousness of the impacts listed in the previous paragraph is dependent on the aerosol concentration and size, but particularly on its chemical composition. It is therefore relevant to distinguish between different aerosol species commonly found in the air:

- Sulfate (SO_4) aerosols originate from sulfur dioxide (SO_2) which has been neutralized by ammonium (NH_4) to form ammonium sulfate ($(SO_4)_2NH_4$, Forster *et al.*, 2007, sect. 2.4.4.1). SO_2 emissions emerge from fossil fuel and, to a much smaller extent, biomass burning, and therefore are vastly considered as anthropogenic. However, small natural contributions originate from volcanoes and the oceans (Haywood and Boucher, 2000);
- Nitrate (NO_3) aerosols originate from nitrogen oxides (NO_x) which has been neutralized by ammonium (NH_4) to form ammonium nitrate (NO_3NH_4, Forster *et al.*, 2007, sect. 2.4.4.5). NO_3 emissions emanate from a variety of sources such as fossil fuel and biomass burning, which is why Delmas *et al.* (1997) estimated that 83% of NO_3 emissions are anthropogenic in nature. Natural sources of NO_3 include bacteria and lightning.
- Particulate organic matter (POM), made up largely of organic carbon (OC), is the result of fossil fuel and biomass burning. The former is an anthropogenic source while the latter can be either a natural or an anthropogenic source. As a whole, sources of POM are widely considered to be anthropogenic (Haywood and Boucher, 2000; Forster *et al.*, 2007, sect. 2.4.4.3);
- Black carbon (BC) particles are the result of incomplete combustion and originate from the same sources as POM (Haywood and Boucher, 2000; Forster *et al.*, 2007, sect. 2.4.4.2);
- Mineral dust (DS) is the product of wind erosion predominantly in arid environments. Sources are therefore considered natural. However, deforestation, agricultural and industrial practices are responsible for a portion of anthropogenic dust aerosols in the atmosphere (Haywood and Boucher, 2000; Forster *et al.*, 2007, sect. 2.4.4.6; Denman *et al.*, 2007, sect. 7.5.1.1).
- Sea salt (SS) aerosols originate from the oceans. The release of salt particles depends on meteorological factors such as surface wind speed and sea surface temperature (Denman *et al.*, 2007, sect. 7.5.1.2).

There is scientific interest in studying aerosol pollution in cities because associated industries and road traffic are major sources of particulate matter and gaseous contaminants capable of forming aerosols through various chemical reactions and physical processes. Cities do offer a wide variety of opportunities such as employment, education, health care, entertainment and other services which stimulate an ongoing and accelerating urbanization movement around the world

(Moore *et al.*, 2003). The United Nations (2014) estimated that 30% of the world's population lived in an urban area in 1950. This proportion grew to 47% in 2000 and is expected to reach 66% in 2050 (United Nations, 2014). Particularly in developing countries, where the rate of urbanization is the greatest (Subbotina, 2004, chap. 10), cities are lacking the means to adjust fast enough to fulfill the demand of its rapidly growing population and economic development. In this respect, urbanization comes with its fair share of environmental consequences (Sharma and Joshi, 2016). The phenomenon known has *global dimming* which consists of a significant decrease in solar radiation flux around the world since the 1950's is actually spatially inconsistent and much more pronounced over densely populated urban areas (Alpert *et al.*, 2005; Alpert and Kishcha, 2008). Indeed, atmospheric aerosol concentrations are significantly higher in populated cities as opposed to rural or remote areas (Cheng and Tsai, 2000), and the cities' population growth in developing countries tends to correlate with an increase of aerosol concentration (Kishcha *et al.*, 2011). Rapid urbanization and development in India and China resulted in a sharp increase of air pollutant emissions during the last decade (Lu *et al.*, 2011) and frequently recurring episodes of air pollution and haziness. On the other hand, urbanization in developed countries, albeit at a slower rate, hasn't had such a negative impact. Developed countries did indeed struggle with severe air pollution issues in the past, but their economic and democratic situation provides them with the means to enforce clean air regulations and develop green technologies. As a result, air quality has significantly improved over the last decades in the United States (Hand *et al.*, 2013), Europe (Vestreng *et al.*, 2007; Tørseth *et al.*, 2012) and Japan (Wakamatsu *et al.*, 2013) even though their population and economy kept on growing.

Several years ago, NASA's Global Modeling and Assimilation Office (GMAO) introduced the Modern-Era Retrospective Analysis for Research and Application (MERRA, Rienecker *et al.*, 2011), a reanalysis tool incorporating satellite and model data to reproduce spatially consistent observations for many environmental variables. While the original MERRA included only meteorological parameters (wind, temperature, humidity, etc.), it has recently been extended to include assimilation of biased-corrected aerosol optical depth (AOD) from the Moderate Resolution Imaging Spectroradiometers sensors (MODIS, Remer *et al.*, 2005) on board the Aqua and Terra satellites, which led to its rebranding now known as MERRAero. Although only total AOD is constrained by MODIS observations, the data assimilation algorithm in MERRAero provides speciated hourly data, with the relative contributions from five of the major aerosol species listed previously. Version 1 of MERRAero doesn't assimilate NO_3 particles. Nevertheless, MERRAero provides an innovative tool to the scientific community to study aerosol pollution issues around the world, especially in regions where reliable surface-based monitoring is scarce or unavailable. Examples of MERRAero's applicability can be found in Kessner *et al.* (2013), Colarco *et al.* (2014), Kishcha *et al.* (2014; 2015) and Yi *et al.* (2015).

In this study, AOD data from MERRAero is used to assess the state of air quality over a large selection of major metropolitan areas around the world (hereafter simply referred to as "cities") over the last thirteen years (2003–2015). Speciation data is used to determine which aerosol species contribute most to AOD over each city and a trend analysis is performed to evaluate how local and regional factors, as well as natural and anthropogenic factors, affect aerosol pollution in urban environments. Alpert *et al.* (2012) previously and similarly analyzed AOD trends over a selection of major cities around the world based on MODIS data. The advantage of using MERRAero as opposed to just MODIS data is its ability to distinguish between aerosol species which provides substantially more information for analysis.

2 Methodology and data

2.1 MERRA Aerosol Reanalysis

NASA's Version 1 of MERRAero incorporates the latest version of the Goddard Earth Observing System (GEOS-5). It contains components for atmospheric circulation and composition (including atmospheric data assimilation), ocean circulation and biogeochemistry, and land surface processes. GEOS-5 also includes an atmospheric particulate matter (PM) module (Colarco *et al.*, 2010, and references therein). This module is based on a version of the Goddard Chemistry, Aerosol, Radiation and Transport (GOCART) model (Chin *et al.*, 2002). GOCART treats the sources, sinks and chemistry of SO_4, OC, BC, DS and SS particles. DS and SS emissions are a function of surface properties and wind speed at the surface. Sources of other species are simulated from emission inventories, including their precursors. SO_2 anthropogenic emissions are input from the Emission Database for Global Atmospheric Research (EDGAR) version 4.1 inventory from 2005 and biomass burning emissions (primarily OC and BC) are input from the NASA Quick Fire Emission Dataset (QFED) version 2.1 (Buchard *et al.*, 2015). PM species are treated as external mixtures and do not interact with each other. MERRAero also assimilates bias-corrected AOD observations from the MODIS sensor on both Terra and Aqua. MERRAero reproduces the concentrations of all five particulate species modeled by GOCART and their relative AOD contributions all over the world every hour with a resolution of 0.5° latitude by 0.625° longitude from mid-2002 to 2015.

A number of MERRAero components have been evaluated in different regions of the world. Its assimilation of AOD has been validated over Africa, South America, Central and Eastern Asia using many remote sensing instruments by Buchard *et al.* (2015); Nowottnick *et al.* (2015) evaluated its aerosol speciation and vertical structure specific to Saharan dust transport using the Cloud-Aerosol Lidar with Orthogonal Polarization (CALIOP); in the United States, the surface concentrations of SO_2, fine PM and its chemical speciation has been thoroughly evaluated by Buchard *et al.* (2014; 2016); in Europe, an evaluation of the surface concentrations of PM, fine PM and some of their chemical speciation has been performed by Provençal *et al.* (2017a); and finally, the surface concentration of fine PM in Israel and Taiwan was carried out by Provençal *et al.* (2017b).

2.2 Method

A selection of 200 of the world's most populated cities was chosen, inspired by Brinkhoff's major agglomerations list (City Population, http://www.citypopulation.de). All the selected cities have a population of at least 2 million inhabitants. Over every one of them, hourly AOD data from MERRAero were extracted for a period of 13 years, from 2003 to 2015, for total and every one of the five aerosol species. It is worth mentioning that MERRAero's resolution is too coarse to capture the urban core of cities. Urban aerosol load is obviously considered in the simulation, but urban grid points are broadly representative of the metropolitan areas, including the urban core and the surrounding suburbs.

A first analysis is performed by averaging the data over the 13-year period over each city and regrouping the cities by geographical region to determine their aerosol signature. A second analysis is performed by averaging the data by year over each city, calculating a regression trend over the 13 years and performing a Student's *t*-test to evaluate the trend's significance at the 90% confidence

level. This will quantify the consequences of rapid urbanization with respect to air quality as well as ascertain the effectiveness of air pollution control over the last decade. The results are presented in map form. All the numerical data used to produce these maps are included in the supplementary material.

3 AOD distributions of aerosol speciation (2003–2015)

3.1 North and Central America

The proportions of aerosol species to total AOD for a selection of major cities in North and Central America are shown in Fig. 1. The reader is referred to the supplementary material for the actual AOD values. Highest urban AOD values are observed in Central and Eastern United States and Canada, ranging from 0.133 in Miami to 0.190 in Houston. Denver is an exception with the lowest mean AOD in the whole region (0.095). The Northeastern United States is highly populated and industrialized, which explains the higher AOD values in Philadelphia (0.190), Cincinnati (0.189), Washington (0.188), New York City (0.187), Pittsburg (0.184), Cleveland (0.181) and St. Louis (0.180). SO_4 aerosols account for a majority (> 50%) of total AOD in most North American cities. This is in line with Hand *et al.* (2012) who mentioned that the Eastern U.S. states emit substantially more sulfur dioxide (SO_2), a precursor of SO_4 aerosols, compared to the other states. Overall, anthropogenic aerosols (SO_4, POM and BC) represent at least 85% of total AOD in all the Northeastern cities. Nevertheless, overall, the mean AOD is relatively low (< 0.2) in all these cities. This is the result of effective air quality regulation in the U.S. known as the Clean Air Act, first adopted in 1970 and significantly amended in 1990. The success of this regulation has been highlighted by many (e.g., Granier *et al.*, 2011; de Meij *et al.*, 2012; Hand *et al.*, 2013; Xing *et al.*, 2013, de Gouw *et al.*, 2014) by documenting a substantial reduction of SO_2 emissions and/or concentration, among other air pollutants, across the U.S. during the last decades. SO_2 emissions and SO_4 concentrations are generally well correlated (Hand *et al.*, 2013; Xing *et al.*, 2013).

Mean AOD values in Orlando (0.157), Tampa (0.152) and Miami (0.133) are among the lowest in the Eastern U.S. with a significantly stronger contribution from SS aerosol to total AOD (from 16% in Tampa to 26% in Miami) given their proximity to the Atlantic Ocean and the Gulf of Mexico, however, Buchard *et al.* (2016) and Provençal *et al.* (2016) documented a substantial overestimation of SS concentrations by MERRAero in coastal areas, therefore these SS proportions are likely overestimated as well.

The mean AOD in west coast cities is lower, from 0.107 in San Diego to 0.124 in Seattle, but the proportions of POM, BC and DS aerosols are higher. These cities are substantially affected by carbon emissions from wildfires occurring periodically in California, as opposed to solely anthropogenic sources. Indeed, Spracklen *et al.* (2007), who modeled OC emissions from summer wildfires in the Western U.S. between 1980 and 2004, concluded that variability of OC concentration in the Western U.S. is largely due to the variability of wildfire emissions. Furthermore, AOD values from MERRAero averaged by month, shown in Fig. 2(a) for Los Angeles, also suggest this to be the case. Aside from an increase caused by DS in spring, POM are largely responsible for the fluctuation of total AOD, particularly during the wildfire season between July and October. By contrast, the fluctuation of SO_4 AOD is barely perceivable. For the sake of comparison, the same graph is shown for New York City (Fig. 2(b)). The wintertime rainy season is also responsible, to a lesser extent, for the seasonal fluctuation. The fluctuations of SO_4 and POM AOD are much more correlated which suggests that carbonaceous aerosols originate largely from

energy consumption in that city. The higher DS proportion in the Western U.S. and Canadian cities is caused by advection of dust originating from the nearby deserts in the Southwestern U.S. and Northwestern Mexico.

The mean AOD in Mexican cities is relatively low (below 0.140) but its speciation signature is similar to Northeastern U.S. cities, dominated by SO_4 and POM aerosols. The Mexican government also implemented successful management programs and incentives to improve urban air quality during the last decades (Molina and Molina, 2004; Parrish *et al.*, 2011). Finally, AOD in Caribbean cities is also low (0.140 or less) but are much less impacted by anthropogenic aerosols. DS and SS compose over 50% of total AOD in Santo Domingo and San Juan. Indeed, the Caribbean receives a large amount of DS originating from the Sahara (Prospero and Mayol-Bracero, 2013).

3.2 South America

The AOD distribution of aerosol speciation for cities located in South America is shown in Fig. 3. The mean AOD for cities in this region is somewhat lower compared to most cities in North America. Lima and Asunción are the only cities whose mean AOD is above 0.160. The speciation distribution is however quite different. The mean AOD in Buenos Aires and in cities of Southern Brazil is dominated by SO_4 and POM aerosols in more or less similar proportions. POM accounts for over half of total AOD in Goiânia, Brasília and Asunción. Deforestation and biomass burning for agricultural purposes in the Amazon rainforest are responsible for such a substantial presence of carbonaceous aerosols in the air (Sena *et al.*, 2013). Indeed, van der Werf *et al.* (2010) estimated that 14.5% of global carbon emissions from wildfires between 1997 and 2009 originate from South America. A synoptic circulation study published by Freitas *et al.* (2005) suggested that smoke plumes from wildfires in the Amazon are generally blown to the south which explains why POM contributes much less to total AOD in cities on the Brazilian east coast.

Fig. 4 compares the monthly averaged AOD between a city strongly impacted from wildfire emissions (Brasilia) and another one west of the Andes that is much less influenced by such emissions (Santiago). Brasilia is clearly affected by biomass burning emissions as shown by a sharp increase of POM, SO_4 and BC AOD during the wildfire season in the fall. Santiago, on the other hand, is slightly impacted by POM in the fall but its AOD distribution is overall dominated by SO_4 aerosols throughout the year. The impact of the summertime rainy season on the aerosol load over the west coast of South America is also clearly illustrated in Fig. 4(b).

3.3 Africa

Fig. 5 displays the distribution of AOD speciation for cities located in Africa. The standout feature of Africa is obviously the Sahara desert which covers most of the northern part of the continent. DS emissions from the desert contribute to high AOD values observed in cities in vicinity of the desert, such as Kano (0.472), Dakar (0.402) and Khartoum (0.389). DS contributes to over 70% of total AOD in these three cities. DS contribute to ~50% of mean AOD in all other cities in Northern Africa. It is important to mention that MERRAero doesn't assimilate AOD data over bright surfaces such as deserts. Therefore, over the source region, the data is constrained primarily by parameterized emissions determined by wind speed. However, the darker surface of cities might have been sufficient to provide assimilated data in and around them.

The region of tropical Africa, south of the Sahara, is characterized by the savannah and rainforest where human-induced wildfires for agricultural purposes is a recurring practice and is an important source of aerosols (Archibald *et al.*, 2009; Eck *et al.*, 2003). Forest preservation initiatives have been implemented in Africa but Mercier (2012) essentially called them a failure. Over 50% of the world's carbon emissions from biomass burning does indeed originate from Africa (van der Werf *et al.*, 2010). Therefore, POM and BC aerosols together contribute to over 73% of total AOD in Kinshasa, 68% in Luanda and 56% in Harare. The influence of biomass burning aerosols diminishes toward South Africa where urban mean AOD is relatively low, from 0.084 in Cape Town to 0.180 in Durban. The aerosol signature in South African cities resemble most that of North American cities.

3.4 Europe, including Russia and Turkey

The AOD proportions for cities located in Europe are shown in Fig. 6. The situation in European cities is, in many respects, similar to that of North American cities: mean AOD is relatively low while SO_4 aerosols contribute to ~50% or more to it in most cities. Europe is indeed a heavily industrialized continent but effective air quality regulations have also been implemented in Europe which resulted in a consistent emission and concentration decrease of various air pollutants, notably PM and SO_2, over the last decades (Vestreng *et al.*, 2007; Granier *et al.*, 2011; Colette *et al.*, 2011; de Meij *et al.*, 2012; Tøseth *et al.*, 2012). Europe is however significantly impacted by the advection of DS originating for the Sahara desert which represents over 10% of total AOD in all European cities in Fig. 6. Cities closer to the Mediterranean Sea are the most impact, which is in line with Barkan *et al.* (2005), Querol *et al.* (2009) and Pey *et al.* (2013) who analyzed Saharan dust transport over the Mediterranean and into Europe. Indeed, DS contributes to over 30% of total AOD in Izmir, Athens, Ankara and Naples, and to higher AOD values observed in cities such as Istanbul (0.206), Monthly averaged AOD values in Naples are offered as an example in Fig. 7 to show how much DS affects the AOD, especially in the spring when DS contributes almost as much as SO_4 to the total.

The mean AOD in cities of the northern and western parts of Europe tends to be lower, for instance in Madrid (0.104), Stockholm (0.119), Birmingham (0.122) and Lisbon (0.126). Even in the megacities of London and Paris, the total AOD is found to be fairly low (0.128 and 0.138, respectively), due to relatively low levels of SO_4 and a substantial reduction of SO_2 concentrations in London and Paris since the 1990's, but also in other European cities (Henschel *et al.*, 2013; Bigi and Harrison, 2010).

3.5 Western and Central Asia

This region includes a selection of cities west of China and Myanmar which are shown in Fig. 8. Cities close to the Mediterranean Sea enjoy a relatively low aerosol load compared to other cities in this region of the world, from an AOD of 0.163 in Damascus to 0.219 in Tel Aviv. The AOD tends to increase toward Pakistan where the mean AOD in all Pakistani cities is above 0.4, except in Rawalpindi where it lies at 0.370. All cities in Western Asia are characterized by the prominent presence of DS particles due to their location in the Middle Eastern deserts. DS accounts for over 40% of total AOD in all cities of Western Asia and close to 70% in Riyadh and Baghdad. The large presence of DS in Pakistani cities is compounded by the significant presence of SO_4 aerosols, which explains their large overall AOD. The mean AOD from SO_4 aerosols is indeed the

highest in the Pakistani cities. Even if SO_4 AOD is lower in the other cities of Western Asia, SO_4 aerosols still provide an important contribution to total AOD in Tehran (41%), Aleppo (38%) and Tashkent (36%).

India is the world's second most populated country. Fig. 8 includes 15 cities in India with a population over 2 million inhabitants. India is also the world's second largest emitter of anthropogenic aerosols. Its recent population and industrialization growth resulted in a constant increase of fuel consumption and emission of SO_2, OC and BC since the 1990's (Lu *et al.*, 2011; Klimont *et al.*, 2013). This results in high AOD values in most Indian cities; mean AOD is above 0.5 in Patna, Delhi, Kanpur and Lucknow. Indian cities are also affected very much so by the advection of DS from nearby sources, especially in the northern part of India. DS aerosols contribute to 40% of total AOD in Jaipur, 38% in Ahmedabad and in Delhi.

3.6 Eastern Asia

This region includes a selection of cities in China, Taiwan, Korea and Japan, which are shown in Fig. 9. China is the most populated country in the world and has recently been surging economically at the cost of deteriorating air quality. Indeed, Chinese cities record some of the highest speciated AOD averages in the world. Out of the 35 Chinese cities shown in Fig. 9, only three cities, Kunming, Ürümqi and Lanzhou, have a mean AOD value below 0.3. This highest mean AOD is observed in Chengdu (0.800), Wuhan (0.709) and Changsha (0.706). China is the world's largest anthropogenic aerosol emitter. Its energy consumption has increased drastically since 2000 as well as its emissions of SO_2, OC and BC (Lu *et al.*, 2011; Wang and Hao, 2012; Klimont *et al.*, 2013). SO_4 aerosols account for the majority of mean AOD (> 50%) in all Chinese cities except for Ürümqi located in the northeast, far away from the densely populated eastern coast. The contribution of carbonaceous aerosols is also quite significant. Residential activities account for ~70% of OC and ~55% of BC emissions in China (Lu *et al.*, 2011). This results in a strong seasonal AOD fluctuation in many Chinese cities. The megacity of Guangzhou is presented as an example in Fig. 10 to highlight how fossil fuel and biomass burning, combined with frequent stagnating weather conditions, create very high levels of pollution in winter and early spring (Zhang and Cao, 2015). Additionally, advection of DS from the Gobi desert in northern China and the Taklimakan desert in Western China, particularly in the spring (Sullivan *et al.*, 2007), is reflected in the higher DS proportions found in cities of Northern China.

Cities in Taiwan, Korea and Japan are not as polluted as Chinese cities, they are nonetheless influenced by emissions and advection of pollutants from China. Lu *et al.* (2010) estimated that a 1% increase of SO_2 emissions in China leads to 1.15% and 0.71% increases in background SO_2 concentrations in South Korea and Japan respectively. The mean AOD is indeed fairly high in Pyongyang (0.436), Seoul (0.412) and Taipei (0.348). The fact that Japan is farther away from China is reflected in its cities' lower AOD values, ranging from 0.250 in Nagoya to 0.295 in Fukuoka. Air quality policies have also been in place since the 1960's in Japan. SO_2 emissions and concentrations decreased substantially since the 1970's (Kanada *et al.*, 2013; Wakamatsu *et al.*, 2013).

3.7 Southeastern Asia and Oceania

Fig. 11 maps the AOD distribution for cities located in Souteastern Asia and Australia. The

highest mean AOD in this part of the world are found in Bangkok (0.280), Jakarta (0.266) and Yangon (0.235). Cities in Indonesia (Jakarta, Bandung and Surabaya) are mostly impacted by SO_4 aerosols (from 58% to 66% of total AOD). Yangon, Bangkok, Saigon, Kuala Lumpur and Singapore are affected by SO_4 and POM aerosols in more or less similar proportions. Deforestation in tropical Asia emits a substantial amount of carbonaceous particles in the air through biomass burning (Chang and Song, 2010). van der Werf *et al.* (2010) estimated that 9.5% of the world carbon emissions from wildfires originate from equatorial Asia. Manila and Cebu City in the Philippines are less impacted by POM and more affected by SS aerosols.

The mean AOD in the three Australian cities is fairly low: 0.093 in Melbourne, 0.095 in Brisbane and 0.113 in Sydney. Like other industrialized countries, Australia maintains air quality guidelines, below those in the U.S. and Europe, which are generally respected (Broome *et al.*, 2015).

4 AOD trends of aerosol speciation (2003–2015)

4.1 Total AOD

The linear trend between 2003 and 2015 for total AOD and for all the cities is mapped in Fig. 12. The color grading is indicative of the level of change with lighter colors indicating an insignificant change. Globally, the AOD is decreasing in a wide majority of cities. The trends are negative in every single city of the Americas, except in Sacramento and Santiago where they are positive but insignificant. The decreases are significant in cities of Eastern Canada and U.S., and the southeastern part of South America. The strongest decreases are observed in Washington and Asunción. Cities where the trend is insignificant tend to be those least affected by SO_4 aerosols, notably on the western coast of Canada and the U.S., in the Caribbean and in Eastern Brazil. Similarly in Europe, the trends are significantly negative in every European city, except in Stockholm, Kiev, Moscow and St. Petersburg where they are negative but insignificant.

Trends in cities of Africa and Western Asia are generally insignificant, either positively or negatively. They are, however, significant and negatively strong (0.004 decrease per year) in the cities of Algiers, Accra, Abidjan, Ibadan, Lagos and Tunis. The situation in India and Bangladesh is quite different, where all cities exhibit a positive trend, many of which are significant and strong (0.004 increase per year).

The AOD is decreasing in most of the 38 cities of China and Taiwan, albeit at an insignificant rate. The trend is nonetheless significant in a few cities and strongly decreasing in three cities of Southern China (Guangzhou, Xiamen and Hong Kong). Guangzhou, one of China's most populated cities, is in fact the city where the AOD trend is the strongest in the world (decrease of 0.0072 per year). The trends are also strongly negative in all Japanese cities and in the North Korean capital of Pyongyang. In Southeastern Asia, the trends tend to be insignificant, with the exception of Manila and Cebu City in the Philippines and Bangkok in Thailand, who exhibit a significant decreasing AOD. Finally, the three cities in Australia display an insignificant AOD decrease.

A similar analysis is performed in the following subsections for the trends of AOD speciation which will provide explanations for the AOD trends observed in Fig. 12. The reader is referred to the supplementary material for the trend values in all the cities in for all species.

4.2 AOD from SO_4 aerosols

SO_4 AOD trends are shown in Fig. 13. The trend is decreasing significantly in most cities of North America, especially in Eastern Canada and U.S., coinciding with the total AOD decrease observed in Fig. 11 and in line with the goals of the Clean Air Act referenced in Sect. 3.1. Over the last decade (2000–2010), SO_4 concentrations decreased in all regions of the U.S. but even more so over the Eastern U.S. (Hand *et al.*, 2012; 2013). Cities in Central and South America experienced insignificant changes in their SO_4 aerosol load, except in Santo Domingo where it significantly decreased and in Santiago where it significantly increased.

In European cities, SO_4 AOD trends are generally decreasing significantly in Western Europe and insignificantly in Eastern Europe. They are increasing in only two cities, Vienna and Ankara, albeit at insignificant rates. This again is the result of effective air quality regulations implemented in Europe where SO_2 emissions and, by extension, SO_4 concentrations have decreased over the last decade (2001–2010; de Meij *et al.*, 2012).

The decrease in North American and European cities was aided by the recent global economic recession. A few authors have dealt with the issue of economic slowdown and air quality, notably Vrekoussis *et al.* (2013) who documented a sharp decrease of various gaseous pollutants over Greece since 2008, Russell *et al.* (2012) who noticed a stronger-than-normal decrease of the NO_2 column over many U.S. cities during the recession and Castellanos and Boersma (2012) who arrived at the same conclusion for the whole of Europe. Our data suggest that SO_4 aerosols were impacted in a similar fashion, as shown in Fig. 14 for a selection of four megacities in the industrialized world. In New York City, the AOD of SO_4 aerosols started to decline in 2007 and took a sharp drop in 2010 before rebounding the following year; SO_4 AOD also suffered a sharp decline in 2010 in London; the AOD decreased in Moscow between 2007 and 2010; and the same variable has been steadily decreasing in Tokyo since 2006 but more steadily since 2008.

SO_4 AOD trends have changed insignificantly in most cities of Africa and Western Asia where SO_4 aerosols generally contribute little to total AOD. There are some exceptions, for instance, Tunis, Algiers, Abidjan, Accra, Lagos and Ibadan where SO_4 AOD trends are significantly decreasing, Kinshasa where it is strongly decreasing and Cairo where it is significantly increasing. Although the trends are weak in cities in the north of India and in Bangladesh, Indian cities are rather unique in the global landscape in the sense that India is the only country where cities experienced a strong increasing SO_4 AOD trend. Tianjin in China is the only other city in the world with such a trend. In fact, the trend is increasing in all but one city in India (Jaipur), albeit insignificantly in three cities, including the megacity of Delhi. This is the likely result of recent industrial development and population growth in India. Lu *et al.* (2011) estimated that SO_2 emissions increased by 35% between 2004 and 2010 in India.

The trend is insignificant in most Chinese cities, positively in the northern part and negatively in the central part. Cities in Southern China experienced a significant decrease, quite strong in some case (Guangzhou, Chengdu, Hong Kong and Nanning). Like India, China has also been experiencing rapid urbanization and industrialization over the last decade. A look at Fig. 13 in deceiving since only a small number of cities reveal an increasing trend, and an insignificant one in most of those cities for that matter. The reason for this is most likely due to emission patterns observed in China. Lu *et al.*'s (2011) estimates of Chinese SO_2 emissions showed little change between 2004 and 2010. However, this is the result of an 11% increase from 2004 to 2006 (peak year) and a slow decrease since then (9% decrease between 2006 and 2010). Other estimates vary

by numbers but all agree with peak emissions in 2006 and a slow decrease since then (Lu *et al.*, 2010; Wang and Hao, 2012; Zhang *et al.*, 2012; Klimont *et al.*, 2013). Implementation of national comprehensive policies by the Chinese government in 2005 has been successful in this respect. The government also took advantage of international events such as the 2008 Beijing Olympics to temporarily and regionally push stricter air quality guidelines (Lin *et al.*, 2013). However, SO_2 emissions and their trends are very disproportionate throughout China (Zhao *et al.*, 2012a; Zhao *et al.*, 2012b). Guangzhou and Beijing are offered as examples in Fig. 15. Guangzhou follows more closely the national trend: peak SO_4 AOD in 2006 and a slow decrease since then, although not continuous. The SO_4 AOD trend in Beijing is fairly stable throughout the period with slight fluctuations.

The significant and occasionally strong SO_4 AOD decrease in all of Japan's cities is due to Japan's air quality policies and to the recession, as mentioned previously, but also due to its position downwind from China. Since peak SO_4 AOD is observed in 2006 in Tokyo (Fig. 15(d)) and in other Japanese cities, coinciding with China's peak SO_4 emissions, it appears that Japan has also benefited from the air quality regulations implemented by the Chinese government. Trends are significantly decreasing in Yangon, Bangkok, Saigon and both Pilipino cities of Cebu City and Manila, while it is insignificant in Kuala Lumpur, Singapore, the three cities in Indonesia and the three cities in Australia.

4.3 AOD from POM and BC aerosols

Since POM and BC particles originate from the same sources, their trend is similar across the cities (Figs. 16 and 17). Carbonaceous aerosols are also the by-product of fossil fuel burning, it is therefore intuitive to observe a decreasing AOD trend in cities where the SO_4 AOD is also decreasing, and vice versa. This is the case for cities in the Eastern U.S., European, Indian and Japanese cities. However, trends for carbonaceous particles and SO_4 don't always parallel since carbon also originate from natural sources such as wildfires, whose contribution can explain the discrepancy between the two. For instance, the variability and recurrence of wildfires in the Western U.S. are largely responsible for the variability of OC concentrations in the same region (Spracklen *et al.*, 2007). Sacramento in California is offered as an example in Fig. 18. POM AOD fluctuates frequently according to the intensity of wildfires, as opposed to SO_4 AOD which barely changes from one year to another. POM AOD has been steadily increasing since 2010, in conjunction with intensifying wildfire activities experienced in California in recent years. The trend was however deemed insignificant by the statistical test. A single episodic series of strong wildfires can also leave a profound impact on a city's aerosol signature. Western Russia was affected by an intense wildfire season during the summer of 2010 (Konovalov *et al.*, 2011), which explains the POM AOD peak in Moscow in 2010 (Fig. 14(c)). This peak is however probably underestimated since occasionally the smoke from the wildfires was so thick that MODIS incorrectly identified it as clouds (van Donkelaar *et al.*, 2011). Mean AOD from the Aerosol Robotic Network (AERONET) observations in Moscow during July and August 2010 were above 1 for many days and reached a daily average peak of 3.6 on August 7 (Huijnen *et al.* 2012). MERRAero's average of 1.5 for the same day pales in comparison. Without this wildfire episode, the POM AOD decrease in Moscow would have been significant.

As mentioned previously, wildfires in the Amazon rainforest are also an important source of carbonaceous aerosols in South America (Sena *et al.*, 2013). POM AOD is decreasing significantly in all both two South American cities, and quite strongly in three cities (Asunción, Porto Alegre

and Buenos Aires). In accordance, deforestation in the Amazon has sharply decreased since 2004 which appears to have been the cause of conservation policies and economic factors (Malingreau *et al.*, 2012) which resulted in a decreased of carbon emissions (van der Werf *et al.*, 2010). Biomass burning also contributes a large amount of carbon aerosols in Equatorial Africa (Eck *et al.*, 2003); the POM and BC trends are however mostly insignificant in cities of that continent except in right below the Sahara where the trends have decreased significantly. Carbon emission estimates also suggest a decrease during the first half of our study period in Northern Hemisphere Africa (Lehsten *et al.*, 2009; van der Werf *et al.*, 2010).

The BC trend in five cities in Northern China (Zibo, Zhengzhou, Tianjin, Shijiazhuang and Beijing) has increased strongly, which doesn't coincide with the POM trend. In Southeastern and Australian cities, the AOD for carbonaceous particles is insignificant in all cities except in Manila and Sydney, where the trend has decreased significantly.

5 Discussion and conclusion

The MERRA Aerosol Reanalysis was used to study urban air pollution issues around the world by using its assimilation of AOD observations and modeled concentrations of particulate matter over a 13-year period (2003–2015). MERRAero's differentiation of particle speciation makes it a unique and innovative tool capable of estimating the AOD of individual aerosol species with a global and constant coverage, unlike remote sensing instruments. This is particularly useful for studying urban air pollution since cities tend to exhibit a heterogeneous composition of aerosols.

The mean AOD was high (> 0.3) in most cities of China, India, the Middle East, Northern and tropical Africa. At the opposite, it was relatively low (< 0.2) in most cities of North America, South America, Europe, Australia and South Africa. The high AOD values observed in Northern African and Western Asian cities are caused mostly by their proximity to large and sandy deserts. Advection of dust also affects cities in India and Bangladesh but the high AOD averages in cities of these two countries is mostly the result of anthropogenic emissions of pollutants from fossil fuel burning activities. Fossil fuel burning is also responsible, for the most part, for the high AOD values observed in Chinese cities. However, advection of dust affects to some extent the AOD in cities of Northern China as well. High AOD averages in cities of tropical Africa are caused by deforestations and biomass burning activities.

Cities in North America, Europe, Japan, Southeastern Asia and Oceania tend to have a relatively low AOD on average, while SO_4 and POM aerosols contribute to it most. Even though fossil fuel consumption is a major source of pollution in those parts of the world, effective air quality regulations have been successful at keeping emissions and, as a consequence, AOD values low over the last decade. Cities in South America and on the west coast of the U.S. are affected by fossil fuel burning but carbon emissions from wildfires contribute a significant proportion to their mean AOD during the summer. European cities are also affected by dust transport from the Sahara.

Overall, SO_4 aerosols represent at least 10% of the mean AOD in all but two of the 200 cities presented in the various maps of this manuscript, those of Dakar in Senegal and Kano in Nigeria, for the only reason that their AOD is overwhelmed by DS particles due to their location close to the Sahara. POM aerosols represent at least 10% of the average in all but 24 cities, mostly located in Northern Africa or Western Asia. The presence of SS aerosols is significant in coastal cities but usually contributes little to the mean AOD.

The AOD decreased significantly between 2003 and 2015 in most cities of Eastern Canada and U.S., Europe and Japan, accompanied by an AOD decrease from SO_4, POM and BC aerosols, a result of effective air quality regulations and the recent economic recession. Cities in South America, most of which have also experienced a significant AOD decrease, owe this decrease to a declining tendency of AOD from POM aerosols due to a slowdown of deforestation activities in the Amazon rainforest. At the opposite, all cities in India and Bangladesh experienced an increase of AOD from SO_4, POM and BC aerosols which was quite strong in some cities due to recent and rapid urbanization and industrialization.

China has also been experiencing a strong urbanization and industrialization movement over the last decades which caused a strong increase in emissions of atmospheric pollutants. China has nevertheless implemented air quality guidelines during our study period which resulted in insignificant AOD trends in most Chinese cities. The regulations are however showing early signs of success with some cities in Southern China experiencing significant and strong decreases of AOD from SO_4 aerosols. The AOD values over Chinese cities are among the largest in the world, China therefore still has a lot of work to do before achieving the standard of other industrialized countries.

Many cities in Africa and all cities of Western Asia have seen little change in their aerosol load. Cities in this part of the world are mostly affected by aerosols originating from natural sources which don't tend to fluctuate significantly on timescales of a year or more. Maps for AOD trends from DS and SS aerosols were not shown or discussed for the simple reason that the trends were relatively weak and/or insignificant in most cities.

As demonstrated in this paper, MERRAero is an innovative tool that provides to the scientific community the means to study a broad range of aerosol pollution issues around the world. Some limitations pertaining to MERRAero are nevertheless worth raising. As mentioned previously, only MODIS AOD over oceans and dark land surfaces are assimilated. Furthermore, no vertically resolved aerosol information is available. NASA's Version 2 of MERRAero, MERRA-2, incorporates other remote sensing instruments, such as the Multi-angle Imaging Spectroradiometer (MISR) and the Aerosol Robotic Network (AERONET), into its reanalysis to mitigate this shortcoming. MERRA-2 is currently being analyzed and results will be reported in forthcoming publications.

Acknowledgments

This study was made with support from and in cooperation with the international Virtual Institute DESERVE (Dead Sea Research Venue) funded by the German Helmholtz Association.

References

Alpert, P., Kishcha, P., Kaufman, Y.J., Schwarzbard, R., 2005. Global dimming or local dimming?: Effect of urbanization on sunlight availability. Geophys. Res. Lett. 32, L17802.

Alpert, P., Kishcha, P., 2008. Quantification of the effect of urbanization on solar dimming. Geophys. Res. Lett. 35, L08801.

Alpert, P., Shvainshtein, O., Kishcha, P., 2012. AOD trends over megacities based on space

monitoring using MODIS and MISR. Am. J. Clim. Chang. 1, 117–131.

Archibald, S., Roy, D.P., van Wilgen, B.W., Scholes, R.J., 2009. Why limits fire? An examination of drivers of burnt area in Southern Africa. Glob. Chang. Biol. 15, 613–630.

Barkan, J., Alpert, P., Kutiel, H., Kishcha, P., 2005. Synoptics of dust transportation days from Africa toward Italy and central Europe. J. Geophys. Res. 110, D07208.

Bigi, A., Harrison, R.M., 2010. Analysis of the air pollution climate at a central urban background site. Atmos. Environ. 44, 2004–2012.

Broome, R.A., Fann, N., Navin Cristina, T.J., Fulcher, C., Duc, H., Morgan, G.G., 2015. The health benefits of reducing air pollution in Sydney, Australia. Environ. Res. 143, 19–25.

Buchard, V., da Silva, A.M., Colarco, P., Krotkov, N., Dickerson, R.R., Stehr, J.W., Mount, G., Spinei, E., Arkinson, H.L., He, H., 2014. Evaluation of GEOS-5 sulfur dioxide simulations during the Frostburg, MD 2010 field campaign. Atmos. Chem. Phys. 14, 1929–1941.

Buchard, V., da Silva, A.M., Colarco, P.R., Darmenov, A., Randles, C.A., Govindaraju, R., Torres, O., Campbell, J., Spurr, R., 2015. Using the OMI aerosol index and absorption aerosol optical depth to evaluate the NASA MERRA Aerosol Reanalysis. Atmos. Chem. Phys. 15, 5743–5760.

Buchard, V., da Silva, A.M., Randles, C.A., Colarco, P., Ferrare, R., Hair, J., Hostetler, C., Tackett, J., Winker, D., 2016. Evaluation of the surface $PM_{2.5}$ in Version 1 of the NASA MERRA Aerosol Reanalysis over the United States. Atmos. Environ. 125, 100–111.

Castellanos, P., Boersma, K.F., 2012. Reduction in nitrogen oxides over Europe driven by environmental policy and economic recession. Sci. Rep. 2, 265.

Charlson, R.J., 1969. Atmospheric visibility related to aerosol mass concentration. Environ. Sci. Technol. 3, 913–918.

Chang, D., Song, Y., 2010. Estimates of biomass burning emissions in tropical Asia based on satellite-derived data. Atmos. Chem. Phys. 10, 2335–2351.

Cheng, M.T., Tsai, Y.I., 2000. Characterization of visibility and atmospheric aerosols in urban, suburban, and remote areas. Sci. Total Environ. 263, 101–114.

Chin, M., Ginoux, P., Kinne, S., Torres, O., Holben, B., Duncan, B.N., Martin, R.V., Logan, J., Higurashi, A., Nakajima, T., 2002. Tropospheric aerosol optical thickness from the GOCART model and comparisons with satellite and sun photometer measurements. J. Atmos. Sci. 59, 461–483.

Colarco, P., da Silva, A., Chin, M., Diehl, T., 2010. Online simulations of global aerosol distributions in the NASA GEOS-4 model and comparisons to satellite and ground-based aerosol optical depth. J. Geophys. Res. 115, D14207.

Colarco, P.R., Kahn, R.A., Remer, L.A., Levy, R.C., 2014. Impact of satellite viewing-swath width on global and regional aerosol optical thickness statistics and trends. Atmos. Meas. Tech. 7, 2313–2335.

Colette, A., Granier, C., Hodnebrog, Ø, Jakobs, H., Maurizi, A., Nyiri, A., Bessagnet, B., d'Angiola, A., d'Isidoro, M., Gauss, M., Meleux, F., Memmesheimer, M., Mieville, A., Rouïl, L., Russo, F., Solberg, S., Stordal, F., Tampieri, F., 2011. Air quality trends in Europe over the past decade: a first multi-model assessment. Atmos. Chem. Phys. 11, 11657–11678.

de Gouw, J.A., Parrish, D.D., Frost, G.J., Trainer, M., 2014. Reduced emissions of CO_2, NO_x, and SO_2 from U.S. power plants owing to switch from coal to natural gas with combined cycle technology. Earth's Future 2, 75–82.

de Meij, A., Pozzer, A., Lelieveld, J., 2012. Trend analysis in aerosol optical depths and pollutant emission estimates between 2000 and 2009. Atmos. Environ. 51, 75–85.

Delmas, R., Serça, D., Jambertm C., 1997. Global inventory of NO_x sources. Nutr. Cycl. Agroecosyst. 48, 51–60.

Denman, K.L., Brasseur, G., Chidthaisong, A., Ciais, P., Cox, P.M., Dickinson, R.E., Hauglustaine, D., Heinze, C., Holland, E., Jacob, D., Lohmann, U., Ramachandran, S., da Silva Dias, P.L., Wofsy, S.C., Zhang, X., 2007. Couplings between changes in the climate system and biogeochemistry, in: Solomon, S., Qin, D., Manning, M., Chen, Z., Marquis, M., Averyt, K.B., Tignor, M. and Miller, H.L. (eds.), Climate change 2007: the physical science basis, Cambridge University Press, Cambridge, pp. 499–587.

Eck, T.F., Holben, B.N., Ward, D.E., Mukelabai, M.M., Dubovik, O., Smirnov, A., Schafer, J.S., Hsu, N.C., Piketh, S.J., Queface, A., le Roux, J., Swap, R.J., Slutsker, I., 2003. Variability of biomass burning aerosol optical characteristics in Southern Africa during the SAFARI 2000 dry season campaign and a comparison of single scattering albedo estimates from radiometric measurements. J. Geophys. Res. 108, 8477.

Forster, P., Ramaswamy, V., Artaxo, P., Berntsen, T., Betts, R., Fahey, D.W., Haywood, J., Lean, J., Lowe, D.C., Myhre, G., Nganga, J., Prinn, R., Raga, G., Schulz, M., van Dorland, R., 2007. Changes in atmospheric constituents and in radiative forcing, in: Solomon, S., Qin, D., Manning, M., Chen, Z., Marquis, M., Averyt, K.B., Tignor, M., Miller, H.L. (eds.), Climate change 2007: the physical science basis, Cambridge University Press, Cambridge, pp. 129–234.

Freitas, S.R., Longo, K.M., Silva Dias, M.A.F., Silva Dias, P.L., Chatfiled, R., Prins, E., Artaxo, P., Grell, G.A., Recuero, F.S., 2005. Monitoring the transport of biomass burning emissions in South America. Environ. Fluid Mech. 5, 135–167.

Granier, C., Bessagnet, B., Bond, T., d'Angiola, A., van der Gon, H.D., Frost, G.J., Heil, A., Kaiser, J.W., Kinne, S., Klimont, Z., Kloster, S., Lamarque, J.F., Liousse, C., Masui, T., Meleux, F., Mieville, A., Ohara, T., Raut, J.C., Riahi, K., Schultz, M.G., Smith, S.J., Thompson, A., van Aardenne, J., van der Werf, G.R., van Vuuren, D.P., 2011. Evolution of anthropogenic and biomass burning emissions of air pollutants at global and regional scales during the 1980–2010 period. Clim. Chang. 109, 163–190.

Hand, J.L., Schichtel, B.A., Malm, W.C., Pitchford, M.L., 2012. Particulate sulfate ion concentration and SO_2 emission trends in the United States from the early 1990s through 2010. Atmos. Chem. Phys. 12, 10353–10365.

Hand, J.L., Schichtel, B.A., Malm, W.C., Pitchford, M., 2013. Widespread reductions in sulfate

641 across the United States since the early 1990s. AIP Conf. Proc. 1527, 495–498.

642 Haywood, J., Boucher, O., 2000. Estimates of the direct and indirect radiative forcing due to
643 tropospheric aerosols: a review. Rev. Geophys. 38, 513–543.

644 Henschel, S., Querol, X., Atkinson, R., Pandolfi, M., Zeka, A., le Tertre, A., Analitis, A.,
645 Katsouyanni, K., Chanel, O., Pascal, M., Bouland, C., Haluza, D., Medina, S., Goodman, P.G.,
646 2013. Ambient air SO_2 patterns in 6 European cities. Atmos. Environ. 79, 236–247.

647 Huijnen, V., Flemming, J., Kaiser, J.W., Inness, A., Leitao, J., Heil, A., Eskes, H.J., Schultz, M.G.,
648 Benedetti, A., Hadji-Lazaro, J., Dufour, G., Eremenko, M., 2012. Hindcast experiments of
649 tropospheric composition during the summer 2010 fires over Western Russia. Atmos. Chem. Phys.
650 12, 4341–4364.

651 Kanada, M., Fujita, T., Fujii, M., Ohnishi, S., 2013. The long-term impacts of air pollution control
652 policy: historical links between municipal actions and industrial energy efficiency in Kawasaki
653 City, Japan. J. Clean. Prod. 58, 92–101.

654 Kessner, A.L., Wang, J., Leby, R.C., Colarco, P.R., 2013. Remote sensing of surface visibility from
655 space: a look at the United States east coast. Atmos. Environ. 81, 136–147.

656 Kishcha, P., Starobinets, B., Kalashnikova, O., Alpert, P., 2011. Aerosol optical thickness trends
657 and population growth in the Indian subcontinent. Int. J. Remote Sens. 32, 9137–9149.

658 Kishcha, P., da Silva, A.M., Starobinets, B., Alpert, P., 2014. Air pollution over the Ganges basin
659 and northwest Bay of Bengal in the early postmonsoon season based on NASA MERRAero data.
660 J. Geophys. Res.: Atmos. 119, 1555–1570.

661 Kishcha, P., da Silva, A., Starobinets, B., Long, C., Kalashnikova, O., Alpert, P., 2015. Saharan
662 dust as a causal factor of hemispheric asymmetry in aerosols and cloud cover over the tropical
663 Atlantic Ocean. Int. J. Remote Sens. 36, 3423–3445.

664 Klimont, Z., Smith, S.J., Cofala, J., 2013. The last decade of global anthropogenic sulfur dioxide:
665 2000–2011 emissions. Environ. Res. Lett. 8, 014003.

666 Konovalov, I.B., Beekmann, M., Kuznetsova, I.N., Yurova, A., Zvyagintsev, A.M., 2011.
667 Atmospheric impacts of the 2010 Russian wildfires: integrating modelling and measurements of
668 an extreme air pollution episode in the Moscow region. Atmos. Chem. Phys. 11, 10031–10056.

669 Lehsten, V., Tansey, K., Balzter, H., Thonicke, K., Spessa, A., Weber, U., Smith, B., Arneth, A.,
670 2009. Estimating carbon emissions from African wildfires. Biogeosciences 6, 349–360.

671 Lin, J.T., Pan, D., Zhang, R.X., 2013. Trend and interannual variability of Chinese air pollution
672 since 2000 in association with socioeconomic development: a brief overview. Atmos. Ocean. Sci.
673 Lett. 6, 84–89.

674 Lohmann, U., Feichter, J., 2005. Global indirect aerosol effects: a review. Atmos. Chem. Phys. 5,
675 715–737.

676 Lu, Z., Streets, D.G., Zhang, Q., Wang, S., Carmichael, G.R., Cheng, Y.F., Wei, C., Chin, M.,

Diehl, T., Tau, Q., 2010. Sulfur dioxide emissions in China and sulfur trends in East Asia since 2000. Atmos. Chem. Phys. 10, 6311–6331.

Lu, Z., Zhang, Q., Streets, D.G., 2011. Sulfur dioxide and primary carbonaceous aerosol emissions in China and India, 1996–2010. Atmos. Chem. Phys. 11, 9839–9864.

Malingreau, J.P., Eva, H.D., de Miranda, E.E., 2012. Brazilian Amazon: a significant five year drop in deforestation rates but figures are on the rise again. AMBIO 41, 309–314.

Mercier, J.R., 2012. Revisiting deforestation in Africa (1990–2010): one more lost generation. Madag. Conserv. Ecol. 7, 5–8.

Molina, L.T., Molina, M.J., 2004. Improving air quality in megacities: Mexico City case study. Ann. N.Y. Acad. Sci. 1023, 142–158.

Moore, M., Gould, P., Keary, B.S., 2003. Global urbanization and impact on health. Int. J. Hyg. Environ. Health 206, 269–278.

Nowottnick, E.P., Colarco, P.R., Welton, E.J., da Silva, A., 2015. Use of the CALIOP vertical feature mask for evaluating global aerosol models. Atmos. Meas. Tech. 8, 3647–3669.

Parrish, D.D., Singh, H.B., Molina, L., Madronich, S., 2011. Air quality progress in North American megacities: a review. Atmos. Environ. 45, 7015–7025.

Pey, J., Querol, X., Alastuey, A., Forastiere, F., Stafoggia, M., 2013. African dust outbreaks over the Mediterranean basin during 2001–2011: PM_{10} concentrations, phenomenology and trends, and its relation with synoptic and mesoscale meteorology. Atmos. Chem. Phys. 13, 1395–1410.

Pöschl, U., 2005. Atmospheric aerosols: composition, transformation, climate and health effects. Angew. Chem. Int. Edit. 44, 7520–7540.

Prospero, J.M., Mayol-Bracero, O.L., 2013. Understanding the transport and impact of African dust on the Caribbean basin. Bull. Am. Meteorol. Soc. 94, 1329–1337.

Provençal, S., Buchard, V., da Silva, A.M., Leduc, R., Barrette, N., 2017a. Evaluation of PM surface concentration simulated by Version 1 of the NASA MERRA Aerosol Reanalysis over Europe. Atmos. Pollut. Res. 8, 374–382.

Provençal, S., Buchard, V., da Silva, A.M., Leduc, R., Barrette, N., Elhacham, E., Wang, S.H., 2017b. Evaluation of $PM_{2.5}$ surface concentrations simulated by Version 1 of NASA's MERRA Aerosol Reanalysis over Israel and Taiwan. Aerosol Air Qual. Res. 17, 253–261.

Querol, X., Pey, J., Pandolfi, M., Alastuey, A., Cusack, M., Pérez, N., Monero, T., Viana, M., Mihalopoulos, N., Kallos, G., Kleanthous, S., 2009. African dust contributions to mean ambient PM_{10} mass-level across the Mediterranean basin. Atmos. Environ. 43, 4266–4277.

Remer, L.A., Kaufman, Y.J., Tanré, D., Mattoo, S., Chu, D.A., Martins, J.V., Li, R.R., Ichoku, C., Levy, R.C., Kleidman, R.G., Eck, T.F., Vermote E., Holben, B.N., 2005. The MODIS aerosol algorithm, products, and validation. J. Atmos. Sci. 62, 947–973.

712 Rienecker, M.M., Suarez, M.J., Gelaro, R., Todling, R., Bacmeister, J., Liu, E., Bosilovich, M.G.,
713 Schubert, S.D., Takacs, L., Kim, G.K., Bloom, S., Chen, J., Collins, D., Conaty, A., da Silva, A.,
714 Gu, W., Joiner, J., Koster, R.D., Lucchesi, R., Molod, A., Owens, T., Pawson, S., Pegion, P.,
715 Redder, C.R., Reichle, R., Robertson, F.R., Ruddick, A.G., Sienkiewick, M., Woollen, J., 2011.
716 MERRA: NASA's Modern-Era Retrospective Analysis for Research and Application. J. Clim. 24,
717 3624–3648.

718 Russell, A.R., Valin. L.C., Cohen, R.C., 2012. Trends in OMI NO_2 observations over the United
719 States: effects of emission control technology and the economic recession. Atmos. Chem. Phys.
720 12, 12197–12209.

721 Sena, E.T., Artaxo, P., A.L. Correia, A.L., 2013. Spatial variability of the direct radiative forcing
722 of biomass burning aerosols and the effects of land use change in Amazonia. Atmos. Chem. Phys.
723 13, 1261–1275.

724 Sharma, R., Joshi, P.K., 2016. Mapping environmental impacts of rapid urbanization in the national
725 capital region of India using remote sensing inputs. Urban Clim. 15, 70–82.

726 Spracklen, D.V., Logan, J.A., Mickley, L.J., Park, R.J., Yevich, R., Westerling, A.L., Jaffe, D.A.,
727 2007. Wildfires drive interannual variability of organic carbon aerosol in the western U.S. in
728 summer. Geophys. Res. Lett. 34, L16816.

729 Subbotina, T.P., 2004. Beyond economic growth: an introduction to sustainable development, 2nd
730 ed. The International Bank for Reconstruction and Development, Washington.

731 Sullivan, R.C., Guazzotti, S.A., Sodeman, D.A., Prather, K.A., 2007. Direct observations of the
732 atmospheric processing of Asian mineral dust. Atmos. Chem. Phys. 7, 1213–1236.

733 Tager, I.B., 2013. Health effects of aerosols: mechanisms and epidemiology, in: Ruzer, L.S.,
734 Harley, N.H. (eds.), Aerosols handbook: measurement, dosimetry, and health effects, 2nd ed. CRC
735 Press, Boca Raton, pp. 565–636.

736 Tørseth, K., Aas, W., Breivik, K., Fjæraa, A.M., Fiebig, M., Hjellbrekke, A.G., Lund Myhre, C.,
737 Solberg, S., Yttri, K.E., 2012. Introduction to the European Monitoring and Evaluation Programme
738 (EMEP) and observed atmospheric composition change during 1972–2009. Atmos. Chem. Phys.
739 12, 5447–5481.

740 United Nations, 2014. World urbanization prospects, the 2014 revision.
741 http://esa.un.org/unpd/wup/CD-ROM/. Accessed 1 December 2015.

742 van Donkelaar, A., Martin, R.V., Levy, R.C., da Silva, A.M., Krzyzanowski, M., Chubarova, N.E.,
743 Semutnikova, E., Cohen, A.J., 2011. Satellite-based estimates of ground-level fine particulate
744 matter during extreme events: a case study of the Moscow fires in 2010. Atmos. Environ. 45, 6225–
745 6232.

746 van der Werf, G.R., Randerson, J.T., Giglio, L., Collatz, G.J., Mu, M., Kasibhatla, P.S., Morton,
747 D.C., Defries, R.S., Jin, Y., van Leeuwen, T.T., 2010. Global fire emissions and the contribution
748 of deforestation, savanna, forest, agricultural, and peat fires (1997–2009). Atmos. Chem. Phys. 10,
749 11707–11735.

750 Vestreng, V., Myhre, G., Fagerli, H., Reis, S., Tarrason, L., 2007. Twenty-five years of continuous
751 sulfur dioxide emission reduction in Europe. Atmos. Chem. Phys. 7, 3663–3681.

752 Vrekoussis, M., Richter, A., Hilboll, A., Burrows, J.P., Gerasopoulos, E., Lelieveld, J., Barrie, L.,
753 Zarefos, C., Mihalopoulos, N., 2013. Economic crisis detected from space: air quality observations
754 over Athens/Greece. Geophys. Res. Lett. 40, 458–463.

755 Wakamatsu, S., Morikawa, T., Ito, A., 2013. Air pollution trends in Japan between 1970 and 2012
756 and impact of urban air pollution countermeasures. Asian J. Atmos. Environ. 7, 177–190.

757 Wang, S., Hao, J., 2012. Air quality management in China: issues, challenges, and options. J.
758 Environ. Sci. 21, 2–13.

759 Xing, J., Pleim, J., Mathur, R., Pouliot, G., Hogrefe, C., Gan, C.M., Wei, C., 2013. Historical
760 gaseous and primary aerosol emissions in the United States from 1990–2010. Atmos. Chem. Phys.
761 13, 7531–7549.

762 Yi, B., Yang, P., Dessler, A., da Silva, A.M., 2015. Response of aerosol direct radiative effect to
763 the East Asian summer monsoon. IEEE Geosci. Remote Sens. Lett. 12, 597–600.

764 Zhang, Q., He, K., Huo, H., 2012. Cleaning China's air. Nature 484, 161–162.

765 Zhang, Y.L., Cao, F., 2015. Fine particulate matter ($PM_{2.5}$) in China at a city level. Sci. Rep. 5,
766 14884.

767 Zhao, B., Wang, S., Dong, X., Wang, J., Duan, L., Fu, X., Hao, J., Fu, J., 2013a. Environmental
768 effects of the recent emission changes in China: implications for particulate matter pollution and
769 soil acidification. Environ. Res. Lett. 8, 024031.

770 Zhao, Y., Zhang, J., Nielsen, C.P., 2013b. The effects of recent control policies on trends in
771 emissions of anthropogenic atmospheric pollutants and CO_2 in China. Atmos. Chem. Phys. 13,
772 487–508.

773

774 **Figure Captions**

775 **Fig. 1.** Proportion of aerosol speciation for a selection of cities in North and Central America.
776 Mean AOD is provided for a few cities. The reader is referred to the supplementary
777 material for such information for all the cities.

778 **Fig. 2.** AOD of total and aerosol species averaged by month in (a) Los Angeles and (b) New York
779 City.

780 **Fig. 3.** Proportion of aerosol speciation for a selection of cities in South America.

781 **Fig. 4.** AOD of total and aerosol species averaged by month in (a) Brasilia and (b) Santiago.

782 **Fig. 5.** Proportion of aerosol speciation for a selection of cities in Africa.

783 **Fig. 6.** Proportion of aerosol speciation for a selection of cities in Europe.

784 **Fig. 7.** AOD of total and aerosol species averaged by month in Naples.

785 **Fig. 8.** Proportion of aerosol speciation for a selection of cities in Western and Central Asia.

786 **Fig. 9.** Proportion of aerosol speciation for a selection of cities in Eastern Asia.

787 **Fig. 10.** AOD of total and aerosol species averaged by month in Guangzhou.

788 **Fig. 11.** Proportion of aerosol speciation for a selection of cities in Southeastern Asia and Oceania.

789 **Fig. 12.** Linear trend for total AOD in all cities between 2003 and 2015.

790 **Fig. 13.** Linear trend for AOD from SO_4 aerosols in all cities between 2003 and 2015.

791 **Fig. 14.** AOD of total and aerosol species averaged by year in (a) New York City, (b) London, (c)
792 Moscow and (d) Tokyo.

793 **Fig. 15.** AOD of total and aerosol species averaged by year in (a) Guangzhou and (b) Beijing.

794 **Fig. 16.** Linear trend for AOD from POM aerosols in all cities between 2003 and 2015.

795 **Fig. 17.** Linear trend for AOD from BC aerosols in all cities between 2003 and 2015.

796 **Fig. 18.** AOD of total and aerosol species averaged by year in Sacramento.

797

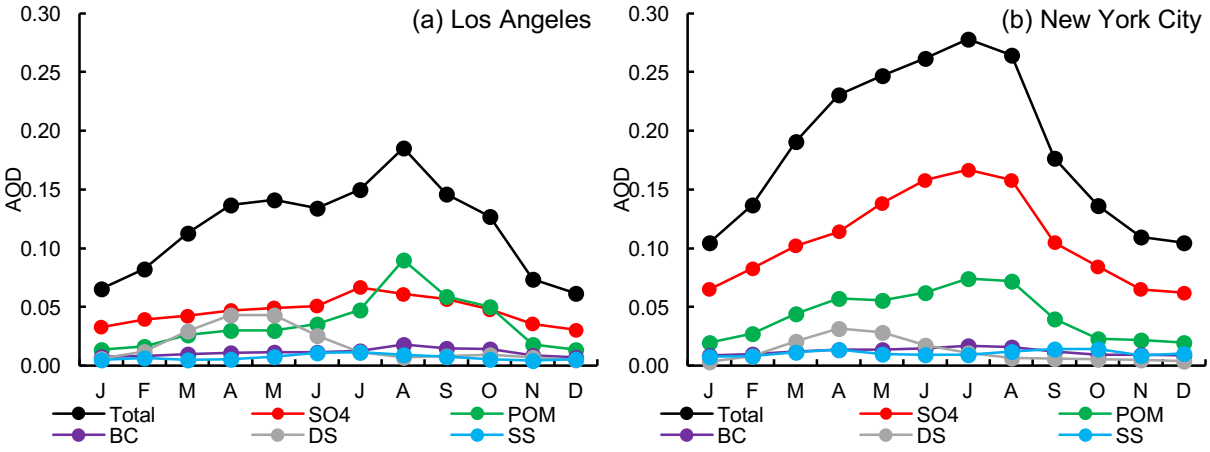

798

799 **Fig. 2**

800

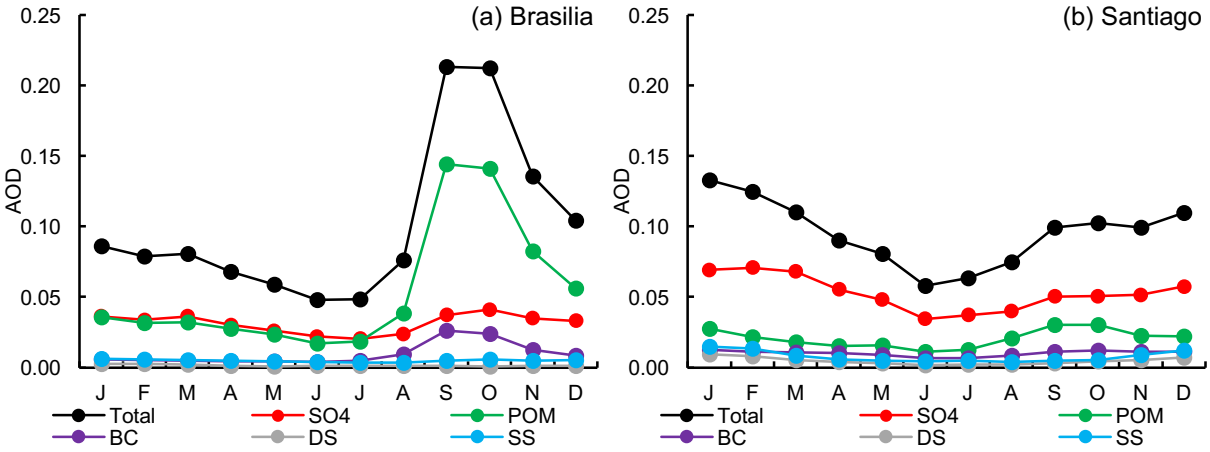

801

802 **Fig. 4**

803

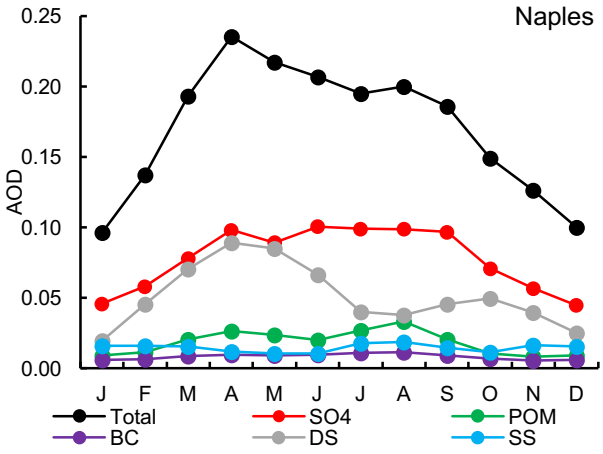

804

805 **Fig. 7**

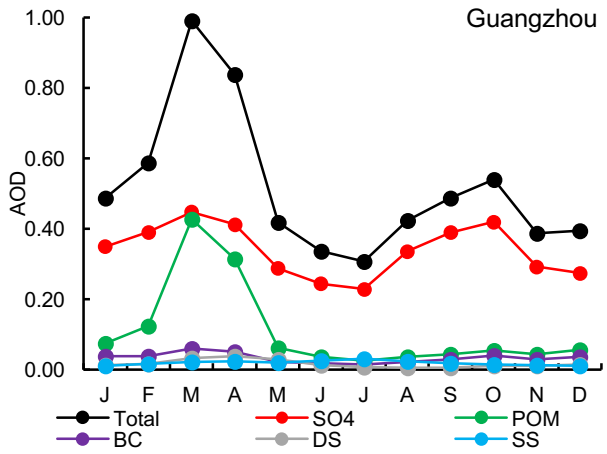

806

807 **Fig. 10**

808

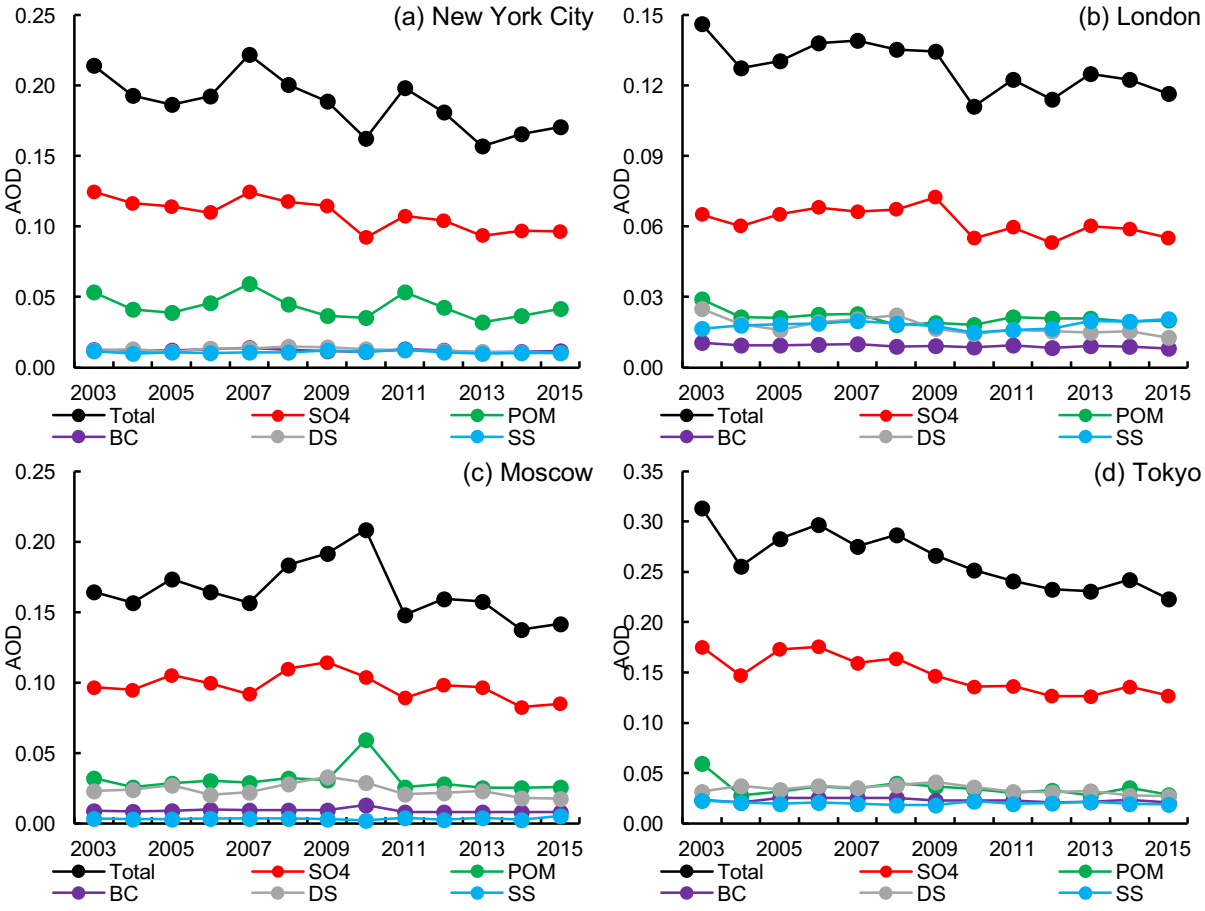

809

810

811 **Fig. 14**

812

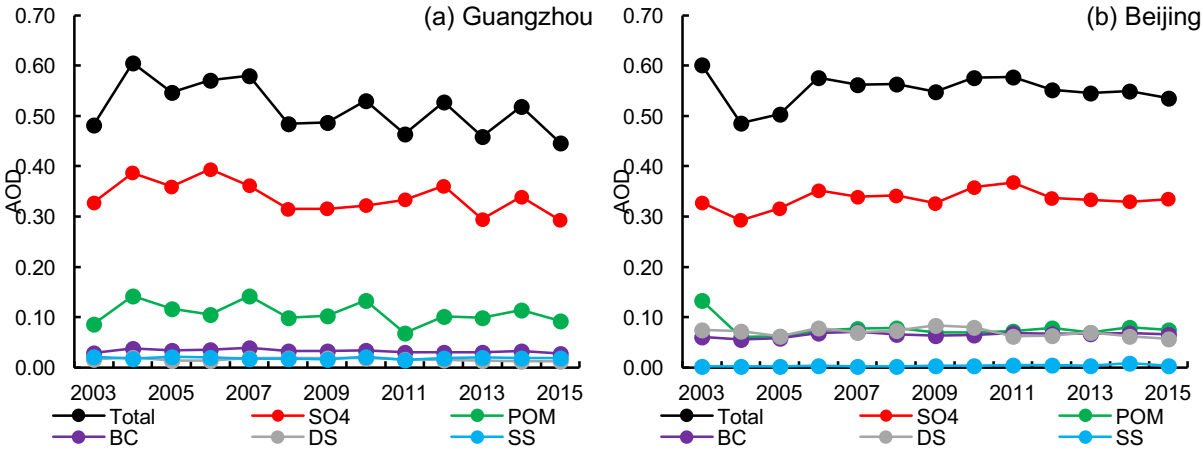

813

814 **Fig. 15**

815

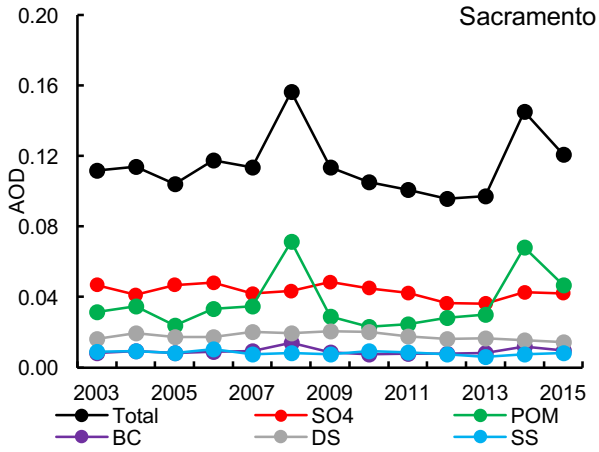

816

817 **Fig. 18**

818

Figure 1

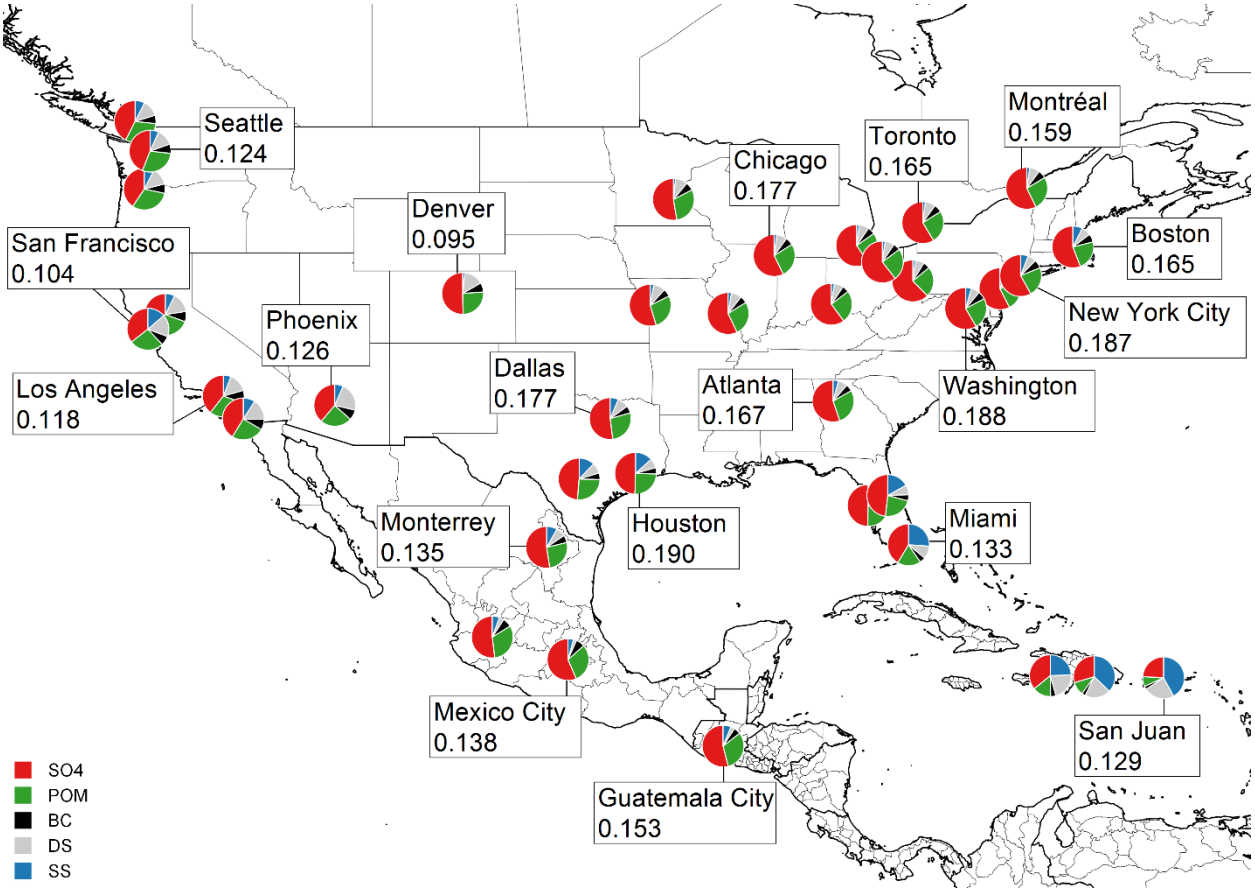
Seattle
0.124
San Francisco
0.104
Los Angeles
0.118
Phoenix
0.126
Denver
0.095
Dallas
0.177
Monterrey
0.135
Houston
0.190
Mexico City
0.138
Guatemala City
0.153
Chicago
0.177
Atlanta
0.167
Toronto
0.165
Montréal
0.159
Boston
0.165
New York City
0.187
Washington
0.188
Miami
0.133
San Juan
0.129
SO4
POM
BC
DS
SS

Figure 3

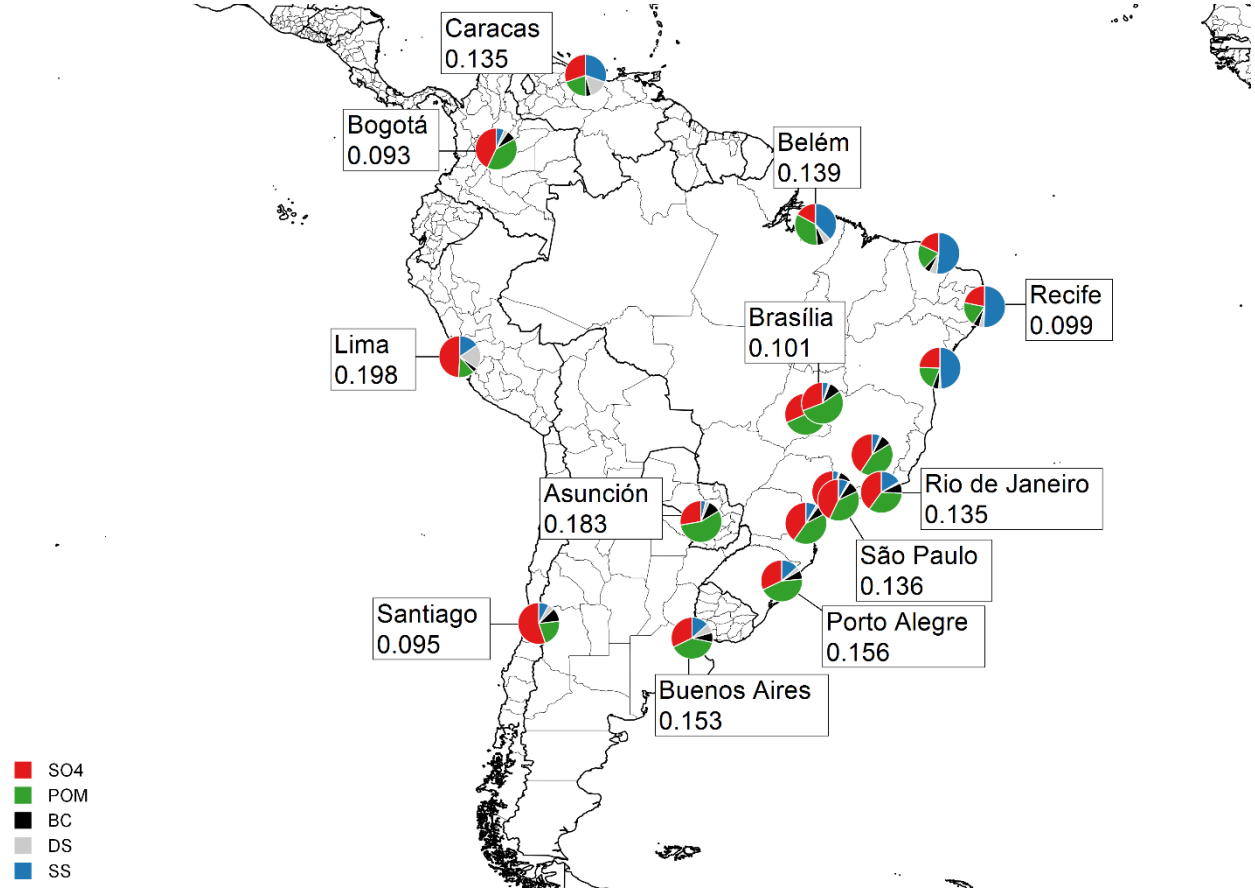
Caracas
0.135
Bogotá
0.093
Belém
0.139
Recife
0.099
Brasília
0.101
Lima
0.198
Asunción
0.183
Rio de Janeiro
0.135
São Paulo
0.136
Santiago
0.095
Porto Alegre
0.156
Buenos Aires
0.153
SO4
POM
BC
DS
SS

Figure 5

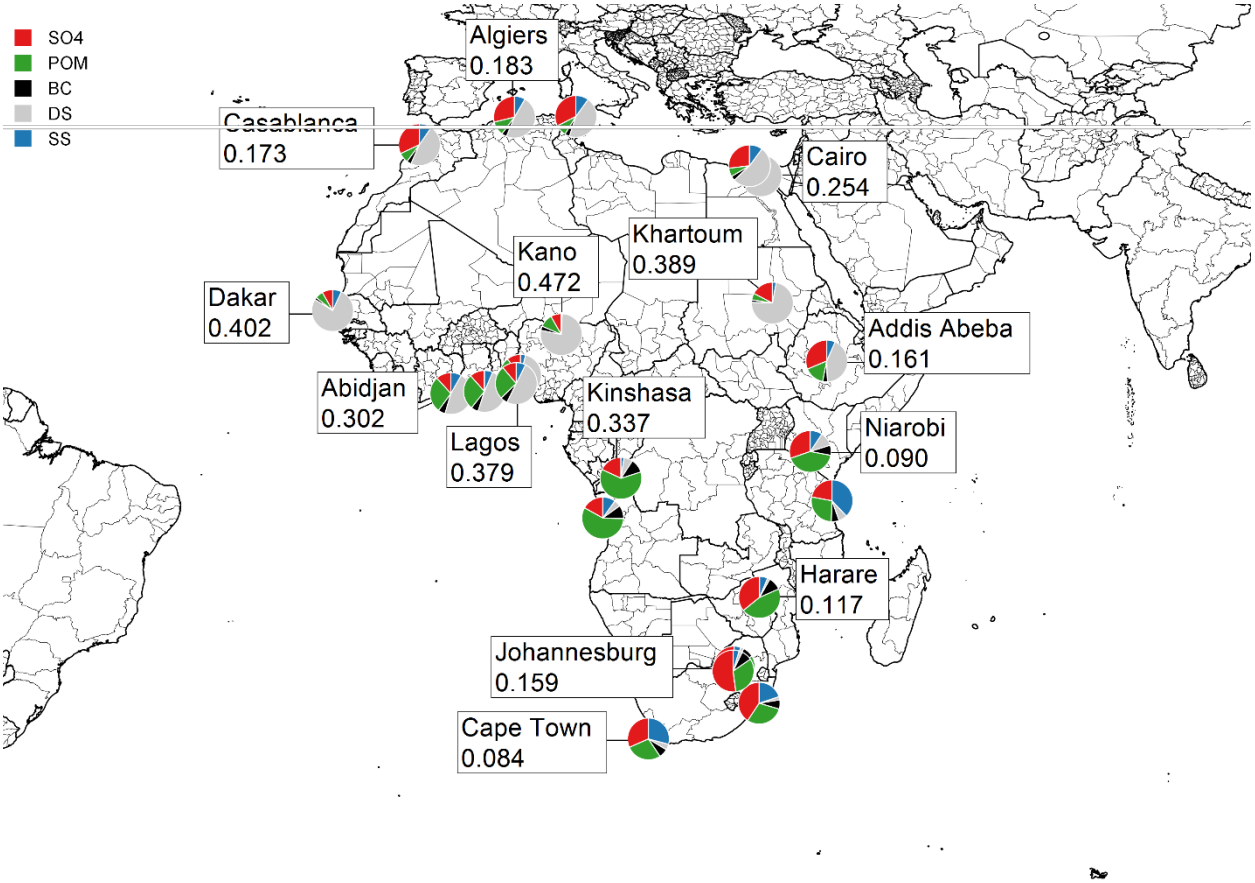
SO4
POM
BC
DS
SS
Algiers
0.183
Casablanca
0.173
Cairo
0.254
Khartoum
0.389
Kano
0.472
Dakar
0.402
Addis Abeba
0.161
Abidjan
0.302
Kinshasa
0.337
Lagos
0.379
Niarobi
0.090
Harare
0.117
Johannesburg
0.159
Cape Town
0.084

Figure 6

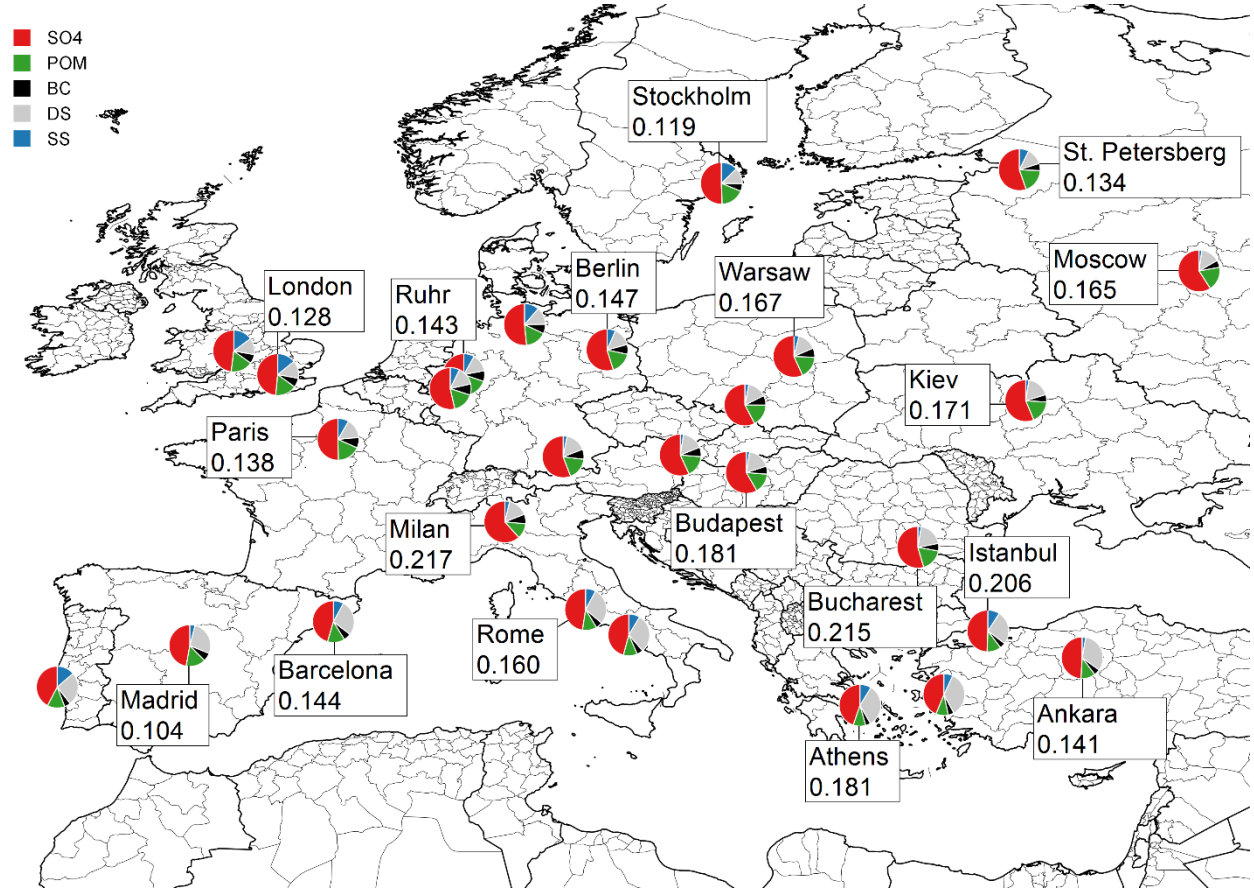
SO4
POM
BC
DS
SS
Stockholm
0.119
St. Petersberg
0.134
Moscow
0.165
Berlin
0.147
Warsaw
0.167
London
0.128
Ruhr
0.143
Kiev
0.171
Paris
0.138
Milan
0.217
Budapest
0.181
Istanbul
0.206
Bucharest
0.215
Rome
0.160
Barcelona
0.144
Madrid
0.104
Ankara
0.141
Athens
0.181

Figure 8

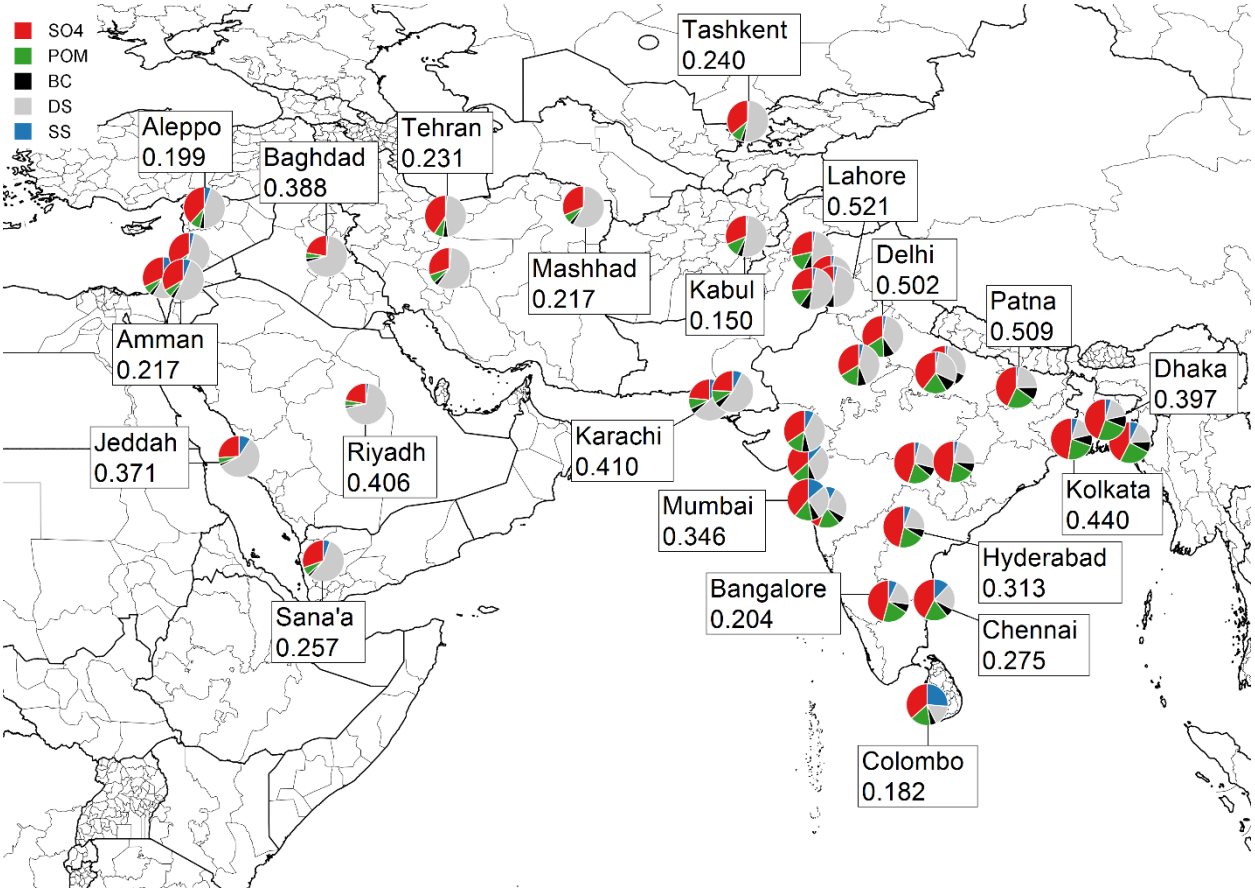
SO4
POM
BC
DS
SS
Tashkent
0.240
Aleppo
0.199
Baghdad
0.388
Tehran
0.231
Lahore
0.521
Mashhad
0.217
Kabul
0.150
Delhi
0.502
Patna
0.509
Amman
0.217
Dhaka
0.397
Jeddah
0.371
Riyadh
0.406
Karachi
0.410
Mumbai
0.346
Kolkata
0.440
Hyderabad
0.313
Bangalore
0.204
Chennai
0.275
Sana'a
0.257
Colombo
0.182

Figure 9

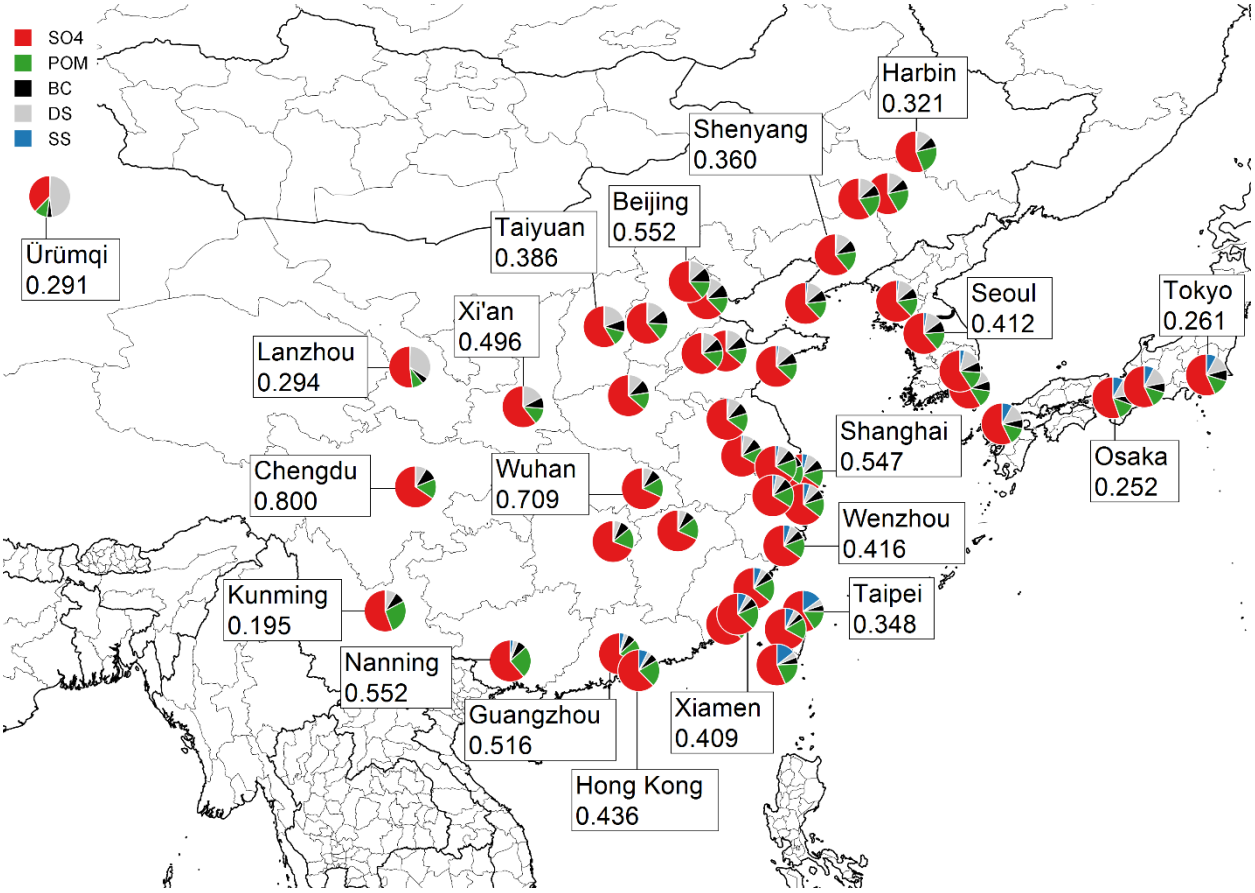
SO4
POM
BC
DS
SS
Ürümqi
0.291
Harbin
0.321
Shenyang
0.360
Beijing
0.552
Taiyuan
0.386
Xi'an
0.496
Lanzhou
0.294
Seoul
0.412
Tokyo
0.261
Shanghai
0.547
Osaka
0.252
Chengdu
0.800
Wuhan
0.709
Wenzhou
0.416
Taipei
0.348
Kunming
0.195
Nanning
0.552
Guangzhou
0.516
Xiamen
0.409
Hong Kong
0.436

Figure 11

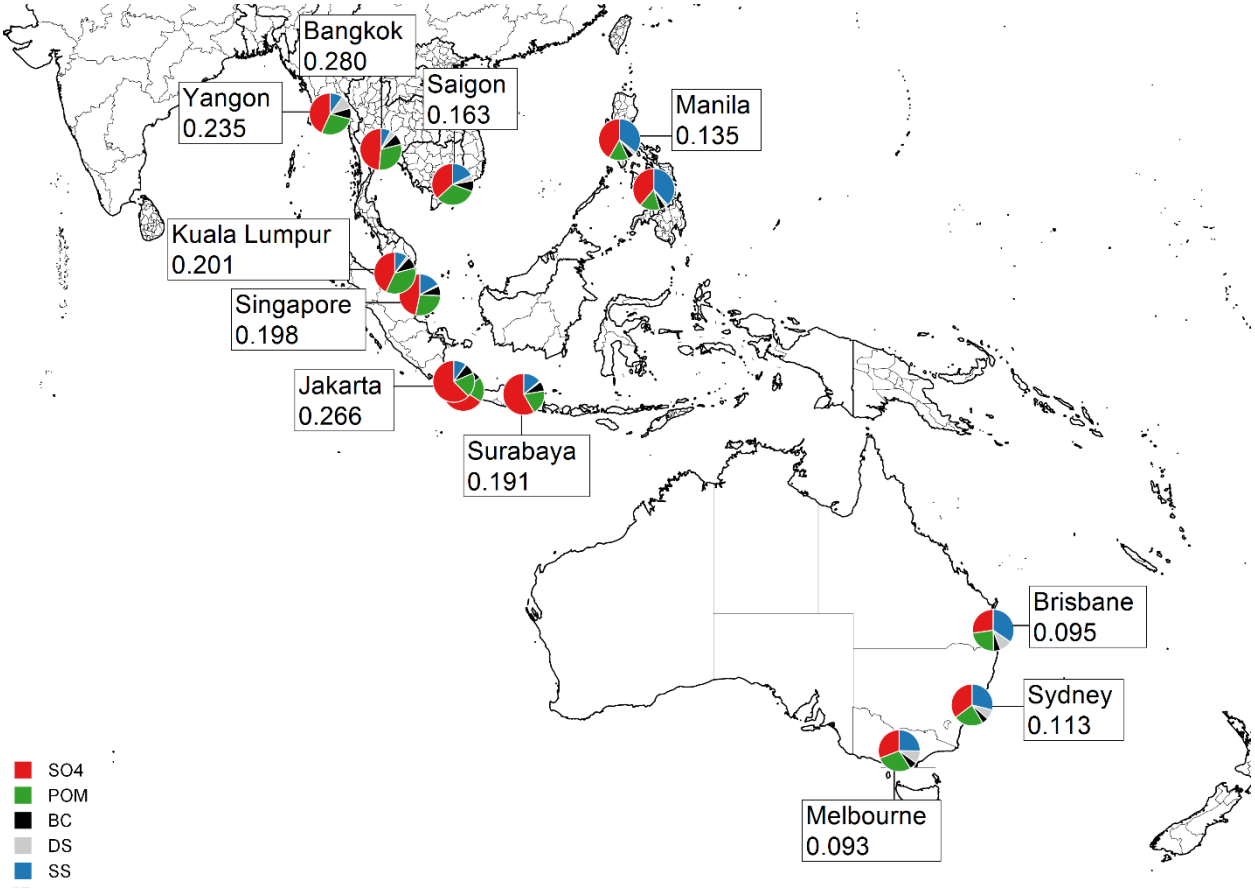
Bangkok
0.280
Yangon
0.235
Saigon
0.163
Manila
0.135
Kuala Lumpur
0.201
Singapore
0.198
Jakarta
0.266
Surabaya
0.191
Brisbane
0.095
Sydney
0.113
Melbourne
0.093
SO4
POM
BC
DS
SS

Figure 12

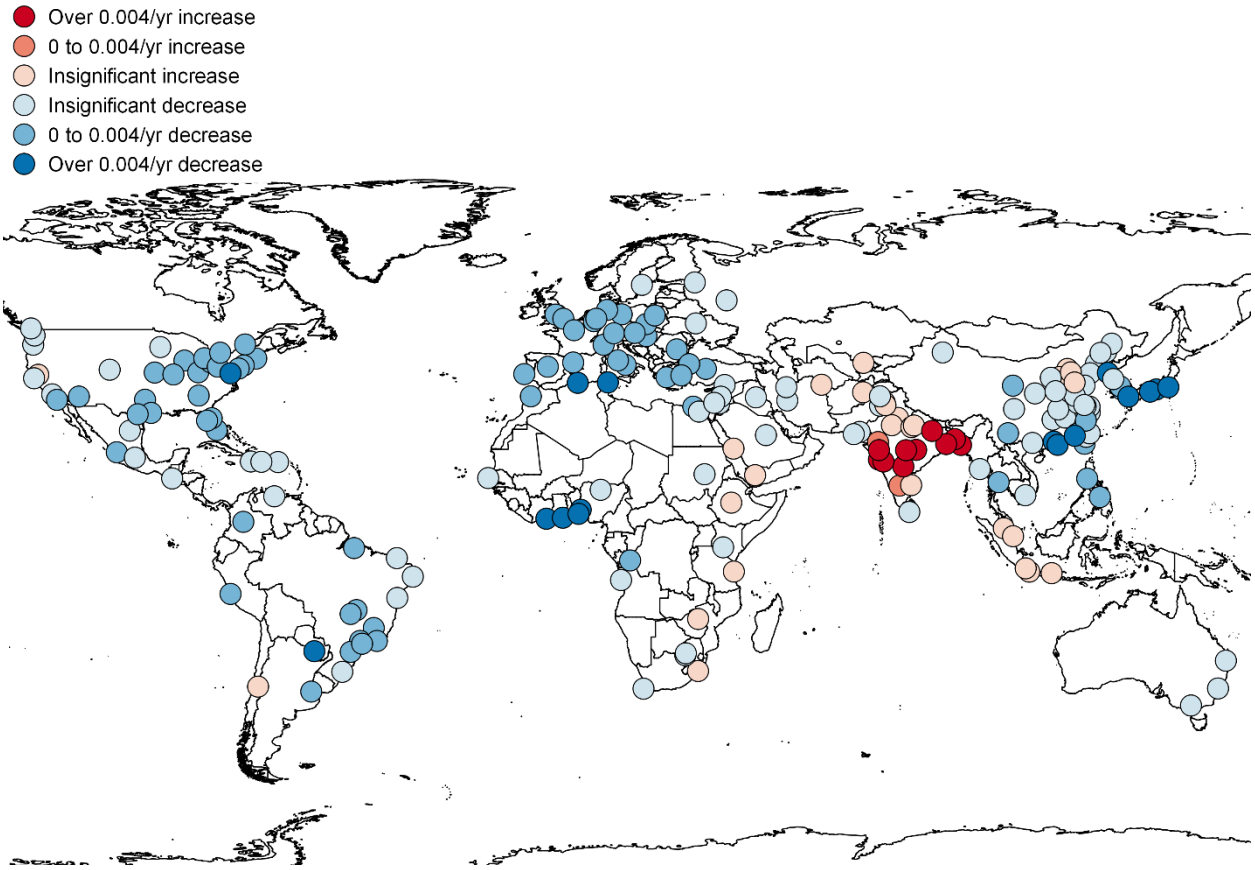
Over 0.004/yr increase
0 to 0.004/yr increase
Insignificant increase
Insignificant decrease
0 to 0.004/yr decrease
Over 0.004/yr decrease

Figure 13

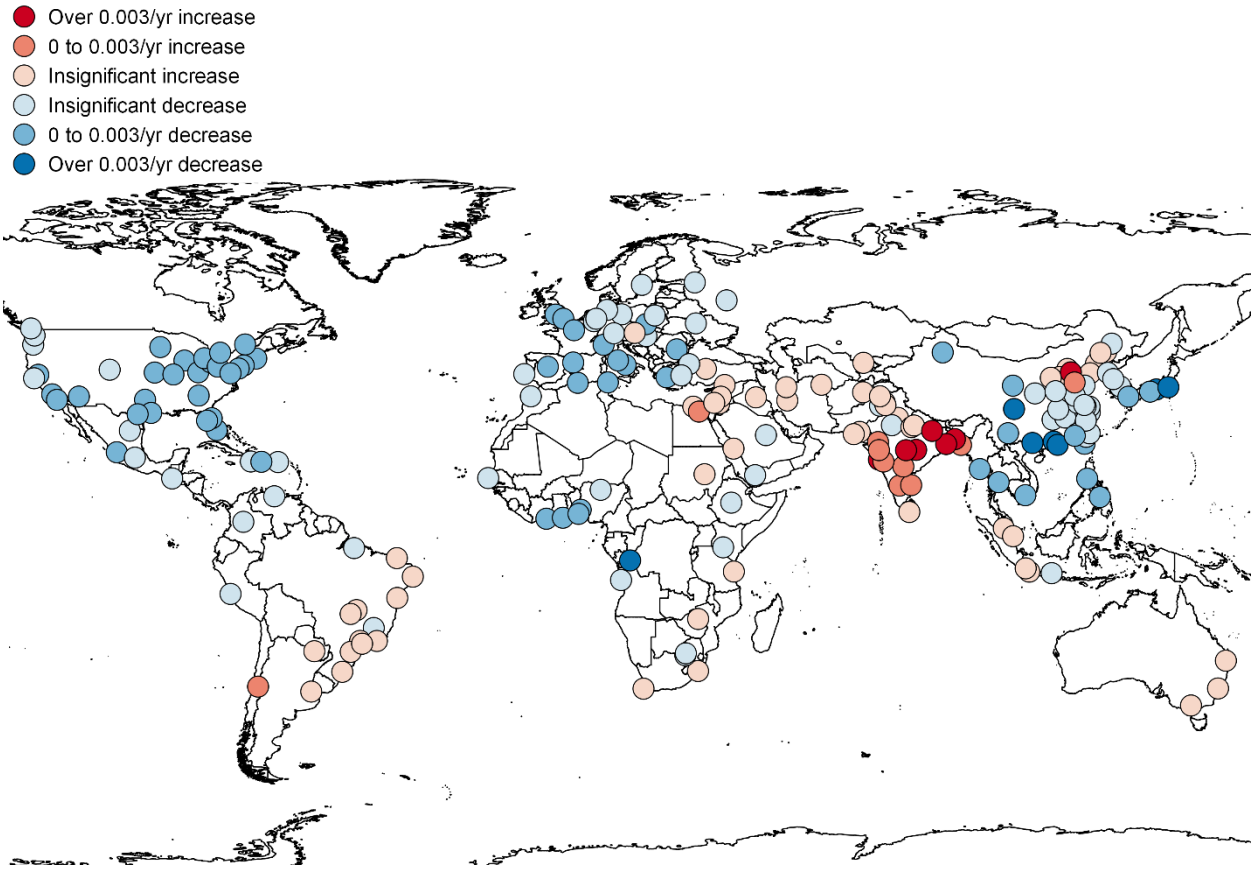
Over 0.003/yr increase
0 to 0.003/yr increase
Insignificant increase
Insignificant decrease
0 to 0.003/yr decrease
Over 0.003/yr decrease

Figure 16

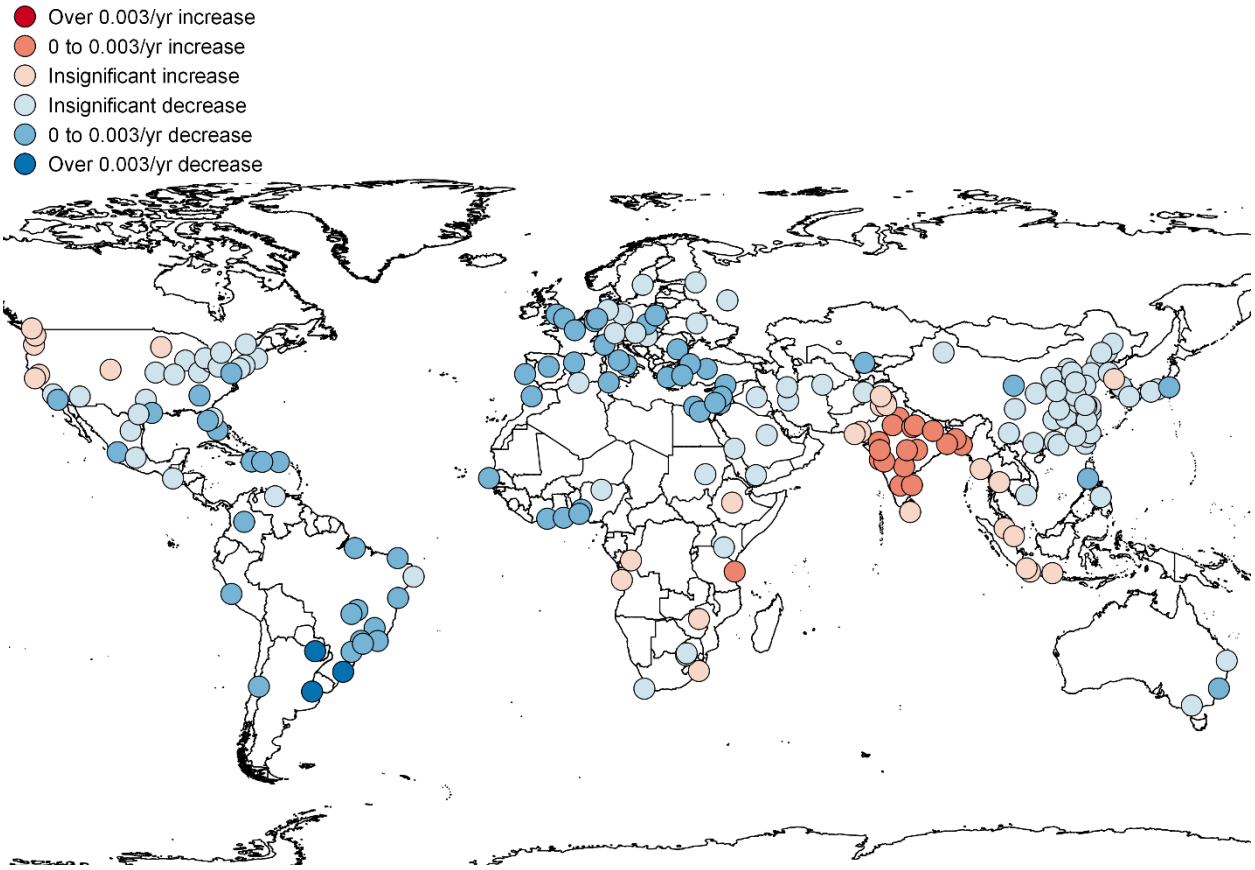
Over 0.003/yr increase
0 to 0.003/yr increase
Insignificant increase
Insignificant decrease
0 to 0.003/yr decrease
Over 0.003/yr decrease

Figure 17

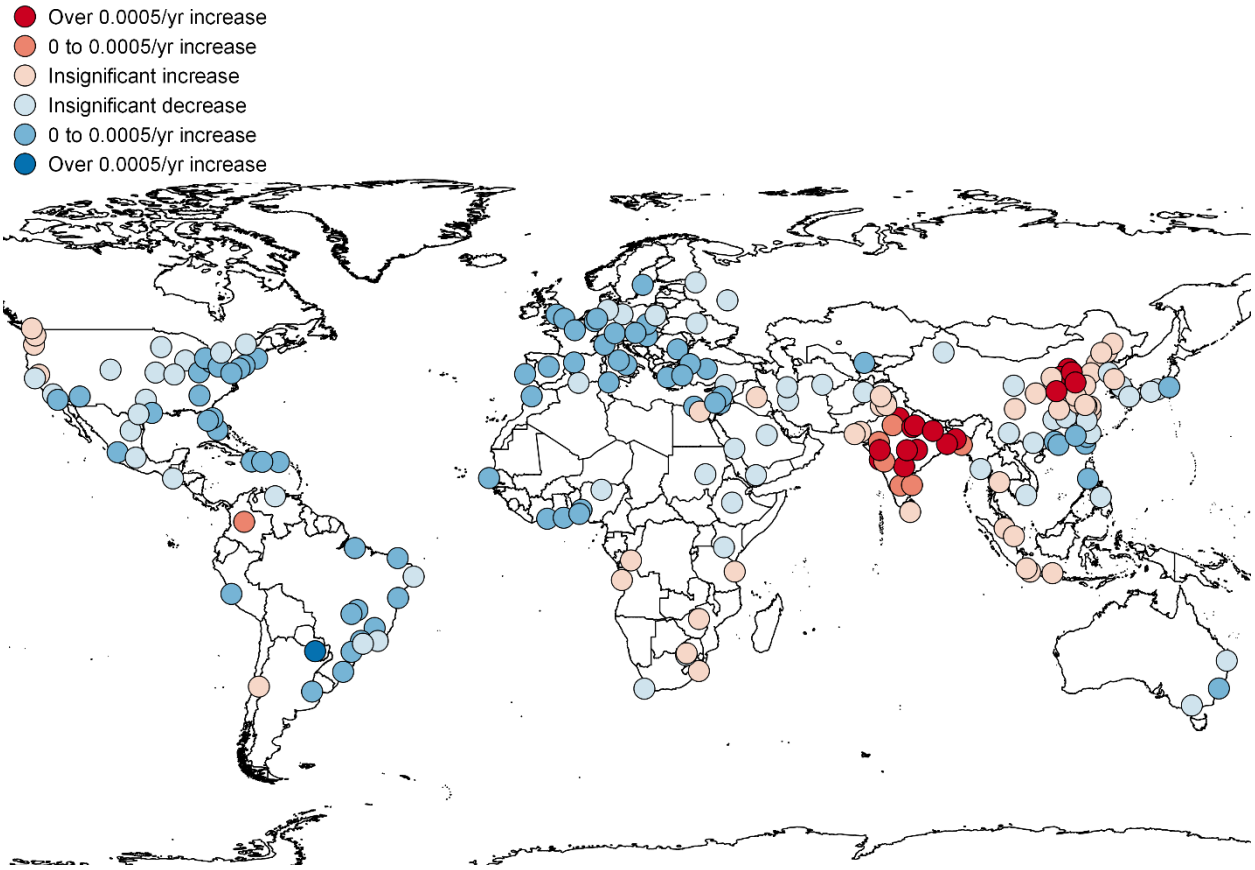
Over 0.0005/yr increase
0 to 0.0005/yr increase
Insignificant increase
Insignificant decrease
0 to 0.0005/yr increase
Over 0.0005/yr increase